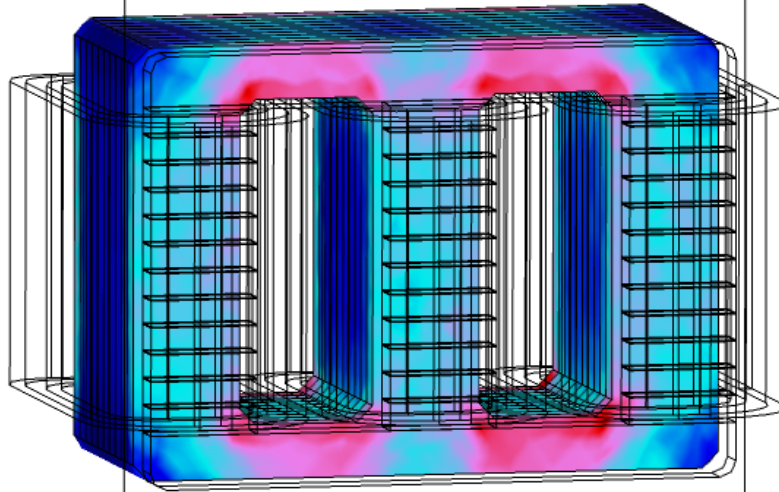




CHALMERS
UNIVERSITY OF TECHNOLOGY



3D modelling and finite element analysis of three phase transformer with integrated inductors in COMSOL Multiphysics

Master's thesis in Electric power engineering

Kunal Choudhary

DEPARTMENT OF Electrical Engineering

CHALMERS UNIVERSITY OF TECHNOLOGY
Gothenburg, Sweden 2021
www.chalmers.se

MASTER'S THESIS 2021

3D modelling and finite element analysis of three phase transformer with integrated inductors in COMSOL Multiphysics

Kunal Choudhary



Department of Electrical engineering
Electric power engineering
CHALMERS UNIVERSITY OF TECHNOLOGY
Gothenburg, Sweden 2021

Kunal Choudhary

© Kunal Choudhary, 2021.

Supervisor: Lars Ronquist, Alstom group

Examiner: Yuriy Serdyuk, Department of Electrical engineering

Master's Thesis 2021

Department of Electrical engineering

Electric power engineering division

Chalmers University of Technology

SE-412 96 Gothenburg

Telephone +46 31 772 1000

Cover: Magnetic field density on the model developed, with increasing intensity as color changes from blue to red.

Typeset in L^AT_EX

Gothenburg, Sweden 2021

3D modelling and finite element analysis of three phase transformer with integrated inductors in COMSOL Multiphysics

Kunal Choudhary

Department of Electrical Engineering

Chalmers University of Technology

Abstract

The use of power electronics in various electrical systems is increasing. The inverters used to switch the DC to AC are widely utilized and usually operate with PWM waveform, resulting in harmonics in the system. This harmonic content leads to increased losses and also introduces electromagnetic interferences into the system and therefore requires additional filtering through LC components.

One of the applications of inverters is in the train wagons, where the DC is converted to 3 phase AC for usage within the train cars. The inverters used are connected to a transformer to obtain the required voltage level. Since there is a limitation of space on board and equipment is needed to be compact, a magnetic integration of inductors and transformer is implemented. This thesis focuses on a 3-dimensional modelling and finite element analysis of a 3 phase 150kVA transformer with integrated inductor core using COMSOL Multiphysics software. A 3D model of the physical transformer is created that includes the series inductance in the form of a shunt core with air gaps along with main core of the transformer, which help in filtering out the harmonic content induced by the inverter. With the simulation model, a frequency domain study of the system is carried out and the evaluation of losses over different operating conditions is performed for the cases with and without utilizing the additional shunt core. With the help of the simulations, early estimation of several parameters to be used in the physical system was conducted. The open circuit and short circuit tests were simulated in the model with desired dimensions, material, study and post processing steps and results were compared with the measurements. It is shown that the modelling provides time efficient, reasonably precise and cheap methodology for the analysis and complements physical experiments.

Keywords: 3D, Transformer, COMSOL, Inductors, Model, Materials, Simulations, electrical.

Acknowledgements

I would like to thank my mentors and supervisor Lars Ronquist, Lennart Zdansky Kruse and Mateusz Rynkiewicz for their support and patience through this work and Petri Syvanen for providing me this opportunity to work. I would also like to thank my examiner Prof. Yuriy Serdyuk for his help on this topic and making me understand things better and Peiyuan chen for initially helping me start this work. My friends and family has been a great support to me during the span of work. I would like to thank my father for everything who left us for heavenly abode midway.

Kunal Choudhary. Göteborg, August 2021

Contents

List of Figures	xi
List of Tables	xiii
1 Introduction	1
1.1 Problem Description	1
1.2 Aim and objectives	2
1.3 Method	3
1.3.1 Software used for Analysis	3
1.4 Outline	4
2 Theory	5
2.1 Basics of transformers	5
2.1.1 Magnetic Core	6
2.1.2 Magnetization	7
2.1.3 Hysteresis loop	8
2.1.4 Permeability	10
2.1.5 Reluctance	11
2.1.6 Air gap	11
2.1.7 Magnetic flux in a transformer	12
2.2 Losses in a transformer	13
2.2.1 Core losses	13
2.2.1.1 Hysteresis Loss	13
2.2.1.2 Eddy Current Loss	13
2.2.2 Copperlosses	14
2.2.3 Steinmetz equation	15
2.3 Magnetic Shunt	15
3 Methods	17
3.1 Geometry	17
3.1.1 Core	17
3.1.2 Shunt Core	18
3.1.3 Windings	20
3.2 Materials	23
3.3 Mesh	26
3.4 Magnetic fields	27
3.4.1 Coils	28

3.4.1.1	Primary Windings	30
3.4.1.2	Secondary Windings	30
3.5	Electric circuit	30
3.6	Study	31
4	Results	33
4.1	Open Circuit test	34
4.2	Open circuit test with shunt core	41
4.2.1	For all frequencies superimposed	42
4.3	Open circuit test without shunt core	42
4.3.1	For all frequencies superimposed	43
4.3.2	Comparison of results with the physical test	43
4.4	Short circuit test	43
4.5	short circuit test with shunt core	50
4.5.1	For all frequencies superimposed	51
4.6	short circuit test without shunt core	51
4.6.1	For all frequencies superimposed	52
4.6.2	Comparison of results with the physical test	52
5	Conclusion	53
	Bibliography	55
A	Appendix 1	I

List of Figures

1.1	System under study(Highlited in Yellow)	3
2.1	Equivalent circuit of an ideal transformer(per phase)	6
2.2	Stacked laminations	7
2.3	Typical magnetization curve	8
2.4	Hysteresis loop	9
2.5	Hysteresis loop with minor hysteresis loops	10
2.6	permeability dependence on saturation	10
2.7	Fringing flux due to air gaps	12
2.8	A snippet showing the flux distortion due to the bolts used for the mechanical stability of the system	13
2.9	Eddy current loop with and without thin sheets with lamination . . .	14
2.10	arrangement of conductors for winding	14
3.1	Core for the transformer model	18
3.2	Shunt core and main core	19
3.3	Air gaps present on shunt core	19
3.4	Winding plane geometry	20
3.5	Winding geometry process	21
3.6	Complete model top view	21
3.7	Complete model front view	22
3.8	Full model	22
3.9	Material properties	23
3.10	BH Curve for Silicon steel GO	23
3.11	Effective BH Curve for Silicon steel GO for frequency domain study .	24
3.12	Range for Effective BH Curve for Silicon steel GO for frequency do- main study	25
3.13	Cycled average for half time cycle	25
3.14	Mesh for the model	27
3.15	Windings of the transformer model	29
3.16	direction of input current in the coil	29
3.17	DY connection	30
3.18	Electrical circuit as in model.	31
3.19	Electrical circuit with filter capacitance.	31
4.1	Magnetic field density on the main core	34
4.2	Magnetic field density mutlislice	35

4.3	Magnetic field density multislice 2	35
4.4	Magnetic field intensity	36
4.5	Loss density	36
4.6	Loss density top view	37
4.7	Electric field around the transformer	38
4.8	Electric displacement around the transformer	38
4.9	Magnetization in the transformer core	39
4.10	Flux density in the shunt core	39
4.11	Magnetic field intensity in the shunt core	40
4.12	Loss density in the windings at open circuit	40
4.13	Surface load density in the transformer	41
4.14	Flux density in the main core at short circuit test	44
4.15	Flux density in the main core at short circuit test	44
4.16	Flux density in the main core at short circuit test top view	45
4.17	Magnetic field intensity in the core	45
4.18	Loss density in the main core at short circuit test	46
4.19	Electric displacement field	46
4.20	Electric field around the transformer during short circuit test	47
4.21	Magnetic field	48
4.22	surface Volumetric loss density in the model	48
4.23	Volumetric loss density in the shunt core of the model	49
4.24	Volumetric loss density in the model view 2	49
4.25	Losses in the transformer model	50
A.1	Selection of transformer components	I
A.2	Geometry steps for main and shunt core	I
A.3	Details of magnetic field interface	II
A.4	Copper properties	II
A.5	Air properties	III
A.6	Silicon properties	III
A.7	Mesh statistics	IV
A.8	Overall steps	IV

List of Tables

3.1	Air gaps	20
4.1	Frequency based open circuit test	41
4.2	Frequency based open circuit test results	41
4.3	Cumulative effect of the frequencies	42
4.4	Frequency based open circuit test	42
4.5	Frequency based open circuit test results without shunt core	42
4.6	cumulative effect of the frequencies	43
4.7	Loss Comparison to physical test results	43
4.8	Frequency based short circuit test	50
4.9	Frequency based short circuit test for 50Hz	51
4.10	Cumulative effect of the frequencies	51
4.11	Frequency based short circuit test	51
4.12	Frequency based short circuit test for 50Hz	51
4.13	Total losses	52
4.14	Loss Comparison to physical test results	52

1

Introduction

Transformer has been a great invention when it comes to Utilisation and transmission of electric power. It is used to link two different voltage levels in a electrical system with the help of a tight magnetic coupling where the windings are electrically isolated.[3] The frequency of the voltage remains the same while the voltages and currents are different. A transformer does not have any moving parts and is static in nature of its operation. Within the electrical domain, transformer is used for the wide span of voltage. Ranging from a use in a small accessory circuit to Ultra high voltage level. The specifications of the transformer are a key feature in the size of the transformer.

Generally transformer are categorized into power transformers, distribution transformers and special purpose transformers by ANSI/IEEE [2]. The special purpose transformer include the transformer like instrument transformer , converter transformers etc. These are named according to the type of utility. One such type of transformer is called Auxillary Transformer. These are used for the purpose of supplying voltage to the low or medium power load ,lighting, heating or as isolating a electrical connection through a magnetic domain.[1]

Throughout the time since its invention, a vast research has improved the operating conditions, materials, reliability and efficiency. For every applications, modifications are required depending on the type of usage.

Due to the introduction of power electronics devices in the system. The power quality has improved but with a cost of variations brought about in the system. Due to use of non linear devices in the converters, the resultant output waveform have higher content of harmonics. [16]

1.1 Problem Description

The transformer for this thesis is called as an 'Auxillary transformer' that is used in the train wagon for indoor power supply within the train cars for the utility of passengers and train staff.

The electrical network for trains is generally of several thousand volts of DC or AC. As most of the services require AC voltage, a subsystem uses an inverter that inverts DC to 3 phase AC. This implementation galvanically isolates the converter side from load side and protects it from harmonics and overcurrents [17]. An onboard transformer also helps in facilitating the voltage level as per the requirement.

The usage of DC- 3 phase Inverter induces harmonics in the system [18] This creates

a distortion in the system fed, produces losses and makes the system inefficient. However a lot of it is reduced by using space vector pulse width modulation [19] but extra LC filtering is also required to limit the frequencies of higher range [18] . A low pass filter is a very good option used to limit the higher order frequencies. This is usually done by the introduction of a LC filter in the configuration at the outputs of the inverter. The Inductance L, provides a higher impedance to higher frequency range and helps filter out the unwanted harmonics in the system.

$$Z_l = j\omega L$$

where,

$$\omega = 2\pi fl$$

The filter capacitor connected in delta configuration is used to filter the unwanted frequencies by allowing a low impedance path for high frequencies to flow. [6] As the Filter inductors and capacitors are on the either sides of the transformer ,therefore it is inevitable that the certain harmonic frequencies flow through the transformer.However the filter capacitors on the secondary side helps them to pass through it , thus avoiding them to reach the load connected on the secondary side.

1.2 Aim and objectives

This thesis aims at modelling the type of above mentioned transformer.As the transformer is mounted on moving wagon, susceptible to cold ,dust,adverse weather conditions and space limitation , a nice approach is to keep it compact and have less parts associated. With this in mind a suitable way is the combined transformer that uses a shunt core to implement the property of inductors within the transformer body domain.

With this modelling, the aim is to

1. Evaluation of parameters like losses and flux density from the specific size of transformer under certain operating conditions.
2. Estimation of transformer components performance.
3. Evaluation of the effects of input base frequency and other input frequencies from the inverter output.
4. Observing the effects of modifying geometry and material properties.
5. Identification of potential hotspots*

With the listed features, the model aims to speed up system design process of the organization.The values from the transformer model can be estimated in the initial stages and analysed with different conditions.This can be a time efficient and cheaper approach in working on a project. If it is wished to get the most of out the model,it can be integrated with software like MATLAB and the established link can work in close coordination of parameters, fetching values back and forth for a more realistic and accurate results. .

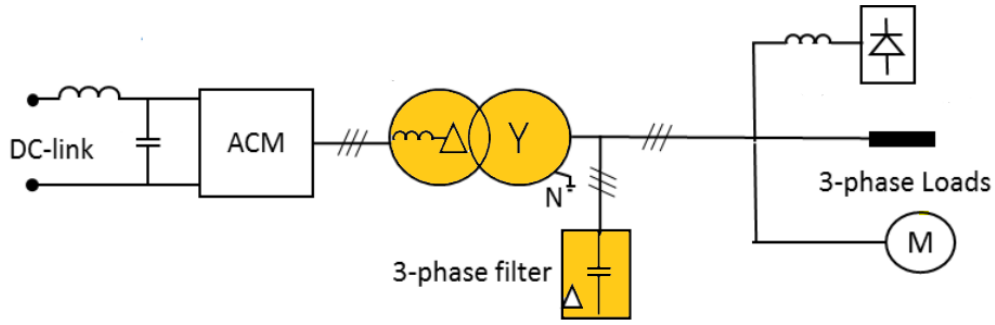


Figure 1.1: System under study(Highlighted in Yellow)

1.3 Method

To carry out this thesis work, the structured steps were followed to get a broader picture of the work being done and keeping it aligned to the research in the field of transformers. An intensive Literature review was the initial phase of this work. This Literature review was helpful in focusing more on a specific subject, narrowing it down to the main components of the transformer in separate approaches. The approach was to keep the model simple with maximum features in use. The most prevalent tool for the transformer simulations is Finite Element modelling using numerical techniques [2]. A suitable software for the modelling setup was chosen as 'COMSOL Multiphysics'. Due to its several features, the usability of this software was very helpful in setting up the model and implementing the specifications required to perform the analysis.

1.3.1 Software used for Analysis

This modelling is done by using the software 'COMSOL Multiphysics' that works on Finite element methods for solutions. The idea to choose this software over other alternatives is due to studies related background and its several advantages known beforehand. [13].

- Simple graphical user interface and application for multiphysics
- Creating and modifying geometries can be done with plenty of options available due to the finite element models.
- The analysis can be performed with the different parameters depending on the type of testing.
- Reduces real life complexities in physical modelling before hand saves time and resources that would have actually been used to develop the physical model.
- Can be used to design custom devices using multiple physics interfaces.
- Setting up base of the model, which can be enhanced and improved at future stages.

This focus of this work is more on modelling this type of transformer so that it is replicated as the almost physical transformer and includes major details of step by step modelling while referring to the available resources.

1.4 Outline

The following sections of the report describe the work carried out to perform this modelling and analysis. The theory section includes the background theory on which the device operation is based. This covers the details about the basics of the transformer and magnetics, design and theory about the transformers in general. The methods section includes the procedure for step by step modelling followed by resulting geometry and view of the model. This includes the necessary modelling steps due to which the model could be successfully Constructed in the software from the beginning.

The results chapter entails the results of the simulations carried out on this model as per the requirements stated in the objectives of this work.

And finally, the conclusion chapter consists the wrap of the work and scopes in the further assessments.

2

Theory

2.1 Basics of transformers

When current is passed through the wire it produces magnetizing force and thus magnetic field around it. The direction of this magnetic flux is given by Fleming's right hand rule, in which the thumb points in the direction of electric current flowing through the wire and the curl of the fingers gives the direction of magnetic flux. The intensity of magnetic field increases if more number of current carrying wires are placed alongside and carrying current in the same direction. The number of turns of the wire is collectively known as coil. The magnetic field passing through an area of cross section gives magnitude of flux.

The relation between the flux density and magnetising force is given by :

$$B = \mu H$$

where,

μ - Permeability

B- Flux density

H- Magnetizing force

Due to this phenomenon rather than producing the flux in the open air or vacuum, suitable materials were discovered in which flux can be made to flow with very less reluctance offered to it. These materials have a high value of permeability and can be magnetised easily. This flux flow in a contained material is the basis of working of a transformer.

Analogous to EMF in electric domain, MMF is for the magnetic domain. The higher intensity of current leads to stronger magnetic fields.

Transformers operate on the principle of electromagnetic induction. The primary and secondary sided cores share the common flux that acts as a working medium which is generated in the coil due to applied alternating voltage on one of the sides. To contain this flux in a material and make it usable to induce voltages in other coil, we require a material with high permeability that helps in the flow of this flux and helps to reduce the flux leaking in the air called leakage flux. [1]. As this flux is alternating in nature, it induces a voltage on the secondary side. The magnitude of this induced voltage depends on the number of turns of the winding connected.

$$V_s = -N \frac{\delta \phi}{\delta t}$$

where,

$\delta\phi/\delta t$ – rate of change of flux

N – Number of turns

Thereby a voltage is induced in the coils at the other side without actually connecting them in electrical domain.

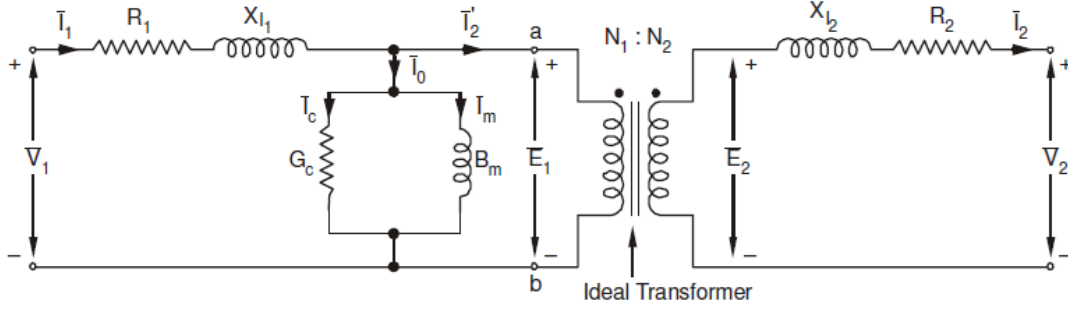


Figure 2.1: Equivalent circuit of an ideal transformer(per phase)

The above figure represents the per phase equivalent circuit of the transformer. The primary side being on the left represented by V_1 . The current in I_1 is the primary side current which energises the transformer core as well as induces alternating flux through the primary turns. This I_1 is the vector sum of I_0 and I_2' , the I_0 is the magnetizing current of the transformer and I_2' is the current that links to the secondary side. For the case of ideal transformer, the magnetising current I_0 is considered to be negligible and full current is assumed to be for the transformer working. The balanced condition for ideal transformer with material having infinite permeability is given by:

$$N_1 \times I_1 = N_2 \times I_2$$

$$\frac{V_1}{V_2} = \frac{N_1}{N_2} = \frac{I_2}{I_1}$$

2.1.1 Magnetic Core

One of the essential parts of a transformer is the core. This is made of magnetic material that has a crystalline structure offering a low reluctance path to the flux that links the secondary and primary windings, and has high permeability property that means higher amount of flux can pass through this material. Thus the concentration of flux in the magnetic material is more than in the surrounding material or air. The magnetic field is increased significantly when a magnetic material is used with the coils carrying current. The Core losses incur major losses which are categorized into Hysteresis losses and Eddy current losses that are described in details in the following sections.

To reduce the effect of eddy currents, the core is not a single piece of material as whole but it is a stack of multiple thin steel of the order of 0.3 or 0.5 mm, to make the core more efficient. These thin laminations are electrically isolated from

each other, so that the circulating current doesn't form up in the transformer and the electrical resistance of the core increases with minimum effect on passage of flux. The limitations of the transformer performances are mostly due to core constraints. The core made up of amorphous material was used for a long time. With the development of material, nowadays silicon steel has come out to be a preferred material for the magnetic core formation.

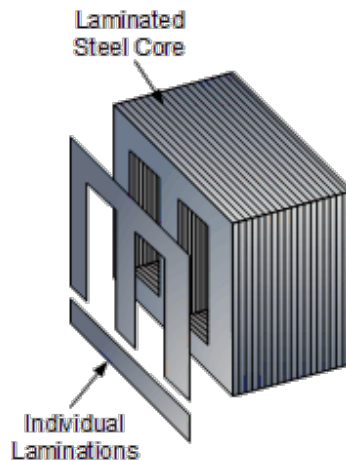


Figure 2.2: Stacked laminations

This system consists of two cores that are specially used for the desired performance. The Cores design is simulated with 'Silicon Steel Grain Oriented' material. This material is available in the inbuilt library of COMSOL, but a few of the properties including material permeability and the electrical conductivity were modified for the analysis in close consideration with the physical material.

Silicon steel is the alloy of iron and silicon that has magnetic properties very suitable to use them in electromagnetic induction applications. The effect of adding silicon to iron is that it makes the material soft and brittle but also reduces the electrical conductivity in the material while decreasing magnetic anisotropy [9]. This helps in reducing the losses in the core.

2.1.2 Magnetization

When a completely demagnetized core is applied with external magnetizing force H , it brings about the change in the flux density of the magnetic material denoted by ' B '.

A typical Magnetization curve is shown in the figure below:

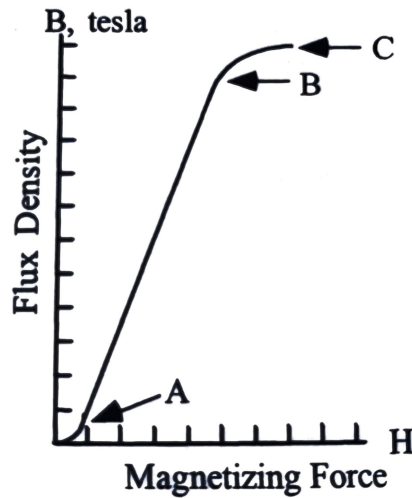


Figure 2.3: Typical magnetization curve

The flux density increases slowly until point A from the zero point as observed in the figure above. The region between point A and B is linear and there is a rapid rise in the flux density until point B. As the flux density is reached to point C, it can be seen that that on further application of magnetizing force, the flux density in the core does not increase and this phenomenon is called saturation of magnetic core. During and after this region, the core accommodation of flux is difficult and it starts to behave like low permeability material such as air.

The magnetic materials are classified into the categories of soft and hard magnetic materials. Soft magnetic materials obtain magnetization properties by being excited by the suitable field and lose the magnetic property as soon as the exciting field is withdrawn. While on the other hand when this excitation is applied to the hard magnetic materials, they retain the magnetization even on removal of excitation.

In electromagnetics, mostly soft magnetic materials are preferred having low coercivity and high permeability. Their main application is for the energy conversion and have brought about a tremendous change in the Power sector and devices used in the world.

2.1.3 Hysteresis loop

A hysteresis loop represents the complete cycle of magnetisation and demagnetisation. It is realised from the actual testing on material and plotted. In most materials the curve is not retraceable, due to the microscopic properties of the domain and some amount of magnetisation remains in the material. This difference in the different values of flux density at the same magnetizing force value is called hysteresis. The width of the B-H curve is used to determine the efficiency of the magnetic material. For electromagnetic applications, the least width of hysteresis loop is desirable so that it is easy to magnetize and demagnetize. While for the permanent magnets, the wider area of hysteresis loop is considered so that they can stay magnetised for long time after removal of magnetizing force.

When the hysteresis is not present in the material, the magnetizing current is in phase with the mutual flux and Linear characteristics are also observed.

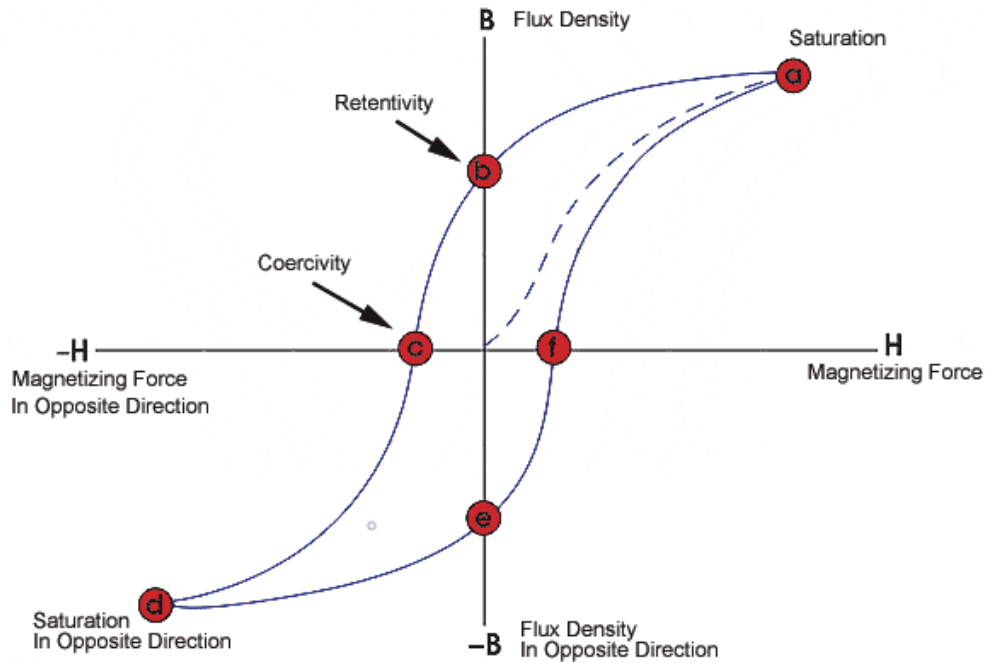


Figure 2.4: Hysteresis loop

Along with the major loops in the circuit, there are some minor loops traced during the observation of properties.

Minor hysteresis loops appear when field with changing amplitude is applied on a demagnetized material. Due to the cyclic nature of this applied field, the different magnetisation cycles are represented, depending on the amplitude of which the path is traced several times, leading to nested loops within the actual Hysteresis curve. The minor loop behaviour is complex to understand, it is produced by the fast operation of magnetic devices the minor hysteresis behaviour in unsaturated material state.[21]. On a research on these minor loops, the positive magnetisation on materials was observed while the applied magnetic field was negative [8]. Due to these characteristics, the results during analysis of magnetic material and their usage can be affected. The minor loops however are not always reproducible due to different microscopic magnetic configuration at unsaturated state even if the macromagnetics are the same. For this work, assumption is made that the losses are not significant due to these minor hysteresis loop in the model. But the effect of the frequencies in the input current to the transformer model is studied for the normal BH Curve data from the material.

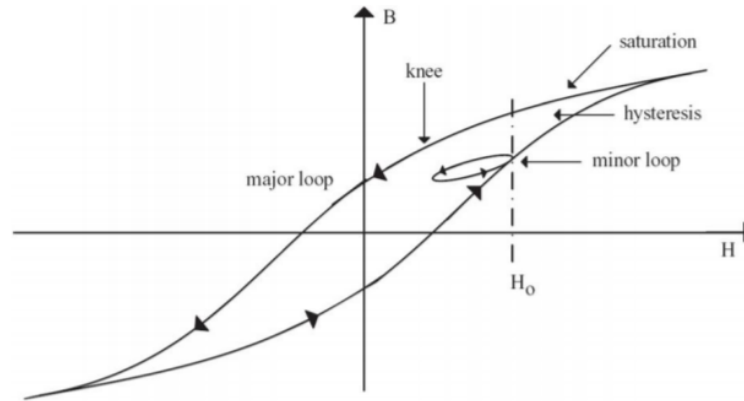


Figure 2.5: Hysteresis loop with minor hysteresis loops

Saturation is the condition of a magnetic material, when on applying the magnetizing force the magnetic field in the material cannot increase after a certain level. The limits of magnetizing can be inferred easily by looking at the magnetization curve of the material. Different materials have different level of magnetization and saturation. As a material starts to get in the state of saturation, permeability of the material starts to decrease from a maximum value and reaches a quite low value. Airgap introduction with constant spacing to increase the level at which saturation reaches in the core.

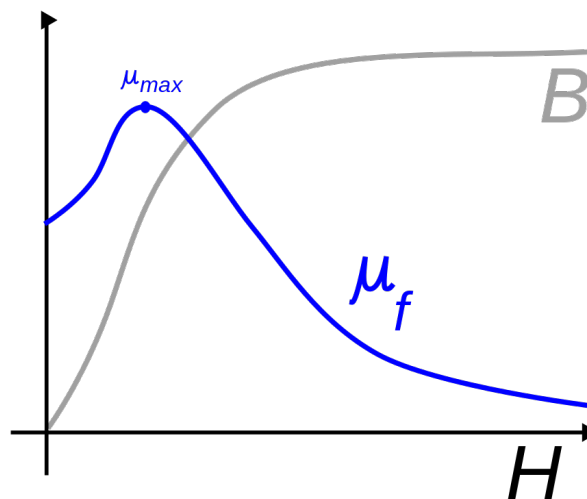


Figure 2.6: permeability dependence on saturation

2.1.4 Permeability

Permeability is the property of a magnetic material that shows how easily it can conduct flux. This is analogous to the conductivity in an electric circuit. More the conductivity of the material, more it is easy for the current to flow in the circuit.

The permeability of the material is given by-

$$\mu = \frac{B}{H}$$

where,

μ - Permeability

B- Flux density

H- Magnetizing force

The higher the permeability of a material, the easier it is to magnetize it and has a lower reluctance for a particular length and cross sectional area.

Silicon steel offers high flux density and the permeability at high flux density is also of good value. For this work, the exact value of permeability is not known beforehand. A suitable assumption for the permeability value referring to the range of permeability for ferromagnetic materials is considered to be around 8500.

2.1.5 Reluctance

Reluctance of a magnetic circuit is analogous to the resistance in the electric circuit. It depends on the properties of the material used and also on the cross section area and design of the magnetic material used. The reluctance of a magnetic circuit can is

$$R_l = \frac{l}{\mu A}$$

where,

R_l - Reluctance

l- Length of magnetic path

μ - Permeability of the material

A - Area of cross section

Therefore when the length and area of cross section is kept constant, the reluctance for a given model is inversely proportional to the permeability of the material used. [12]

2.1.6 Air gap

The presence of air in the magnetic path of the flux in the magnetic materials is termed as air gap. presence of air gaps in the magnetic material alter the effective permeability of the material and can also lead to flux distortion.

Constant air gaps can be introduced to magnetic material used for electromagnetic conversion for storing energy in magnetic domain by which it behaves like an inductor.

In practice there are some intentional core air gaps used in the shunt core of the model discussed. It is not possible to hold the material for a desired air gap, therefore an low permeability material is placed for the specific air gap size.

The total reluctance for the circuit is the reluctance of the magnetic domain and the reluctance of the air gaps combined

Reluctance for the air gap is given by :

$$R_g = \frac{l_g}{\mu_o A_g}$$

where,

R_g - Reluctance of air gap

l_g - Length of air gap

μ_o - Permeability of the material of gap or air

A - Area of cross section of gap

2.1.7 Magnetic flux in a transformer

The flux in the transformer requires an obstruction free path for the perfect working. The distortion in flux can occur in the domain due to poor joints in the stacking and material deformities.

For this work the core gaps are assumed to be minimum and the effect of fringing flux is considered negligible.

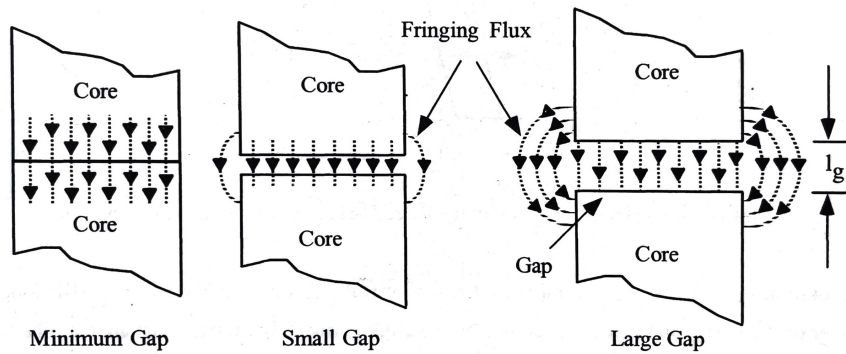


Figure 2.7: Fringing flux due to air gaps

The core and yoke is required to be tightened with the casing and clamps of the transformers for the mechanical stability of the system. The usage of bolts and clamps also affect the flux path in the core material.

The distortions in the main flux can lead to ineffective usage of the system and localised hotspots and losses.

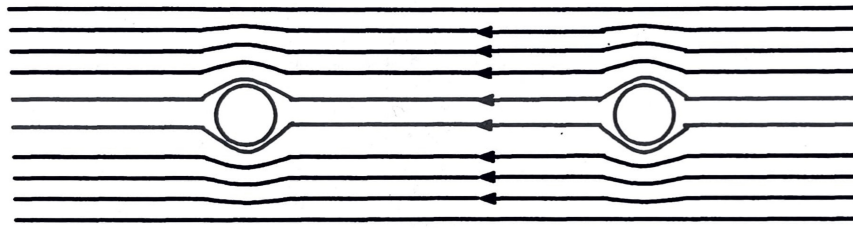


Figure 2.8: A snippet showing the flux distortion due to the bolts used for the mechanical stability of the system

2.2 Losses in a transformer

The elements and material used in a transformer accounts for the losses in transformers. As the device is stationary, therefore no moving part of friction losses are present. These losses are caused due to Current flowing through the coils during working and the alternating magnetic field. These losses are subdivided into constant and variable losses. The constant losses are the ones that remain almost same when the transformer is on no load or full load. While the variable losses are the ones which are dependent on the loading of the transformer and thereby the Current flowing through the circuit.

The technological advancements have helped in reducing the losses to a very low value for the core and its material. The thin stack of laminations and the process of making the material for the core has had a significant impact on the cost of using transformers and reducing losses.

2.2.1 Core losses

2.2.1.1 Hysteresis Loss

For every cycle of excitation of a transformer core, magnetization and demagnetization happen alternatively. For a particular cycle, the magnetic domains of the material are aligned in a direction. On reversal of the cycle, the magnetic domain does not instantly change into the direction of reversal. This can also be defined as the lag in magnetisation of the magnetic material with magnetic field. This leads to losses as heat in the core of the transformer. The wider area of the Hysteresis loop, represents more core losses in the transformer.

2.2.1.2 Eddy Current Loss

During the working of a transformer, the magnetic field is continuously alternating due to the nature of the current by which it is excited i.e AC. This continuously alternating magnetic field induces circulating current in the core of the transformer. If the core is made up of a single piece then the circulating current will make a big loop and contribute to a major loss as heating in the core. To overcome this issue, the core is stacked up of multiples of thin sheets of the material which are insulated from each other. The basic idea behind this is explained in the figure below.

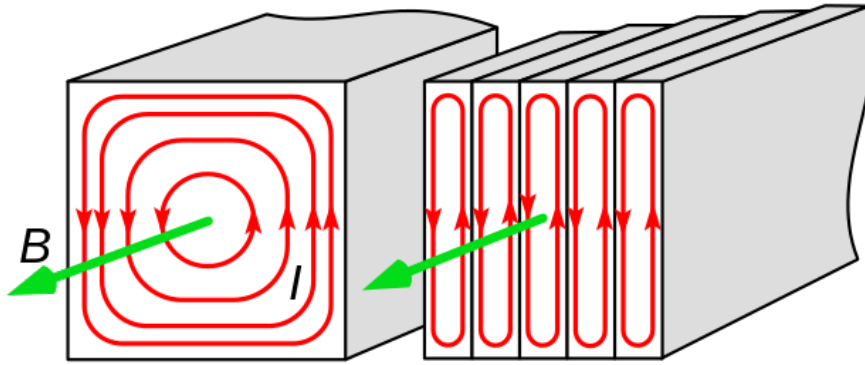


Figure 2.9: Eddy current loop with and without thin sheets with lamination

The eddy current losses in the core are dependent on the frequency of the supply voltage, the thickness of the lamination and maximum flux density in the core.

However the eddy currents are not only confined to the core of the transformer, the surrounding materials like the clamps and bolts can also exhibit the eddy current losses due to the circulating current loops.

2.2.2 Copperlosses

Copper losses are also a major part of the losses occurring in the transformer. These losses are generally ohmic losses happening due to the resistivity of the conductors and energy is dissipated as heat. Since large amount of copper is used to make the primary and secondary windings constituting multiple number of turns. As the eddy currents are discussed for the core, the eddy currents are inevitable in the conductor material also. Rather than taking a thick conductor for winding, the winding conductors are subdivided in to parallel conductors. one such method is the arrangement of conductor stacking with thin insulation between them and a thicker insulation as whole outside. These are known as bunch conductors. Another approach is the Continuously transposed cable conductor CTC, in which a very low thickness off conductor cross section is used and the conductors are transposed at regular intervals for the length of windings.

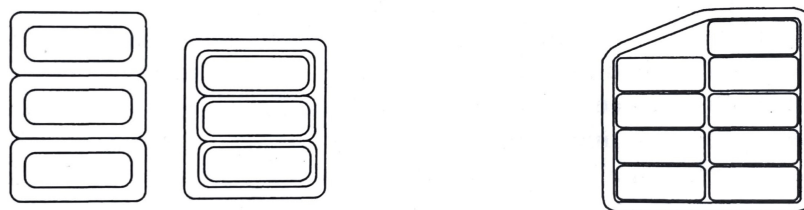


Figure 2.10: arrangement of conductors for winding

2.2.3 Steinmetz equation

Steinmetz equation is used to calculate core loss per unit volume in the magnetic material when it's subjected to sinusoidal flux.

$$P_v = k f^a B^b$$

P_v – Power loss per unit volume

f – frequency

B – Peak magnetic flux density

k, a, b – Steinmetz coefficient.

Steinmetz coefficient k, a and b are found by the curve fitting of the material's available BH curve. As this equations works well for sinusoidal flux, a generalised equation for calculations of losses calculated by non sinusoidal flux was proposed that works on steinmetz parameters with modifications. [14]

The material used in COMSOL doesn't include full hysteresis loop into effect. It constitutes an average B-H curve that includes saturation into effect in the first quadrant of operation. A trial with assumptions is made to implement this steinmetz equation and calculate the losses by a simple calculation with the parameters value taken from the model outputs. The losses however maynot be correct and accurate, but could be advanced furthur with the proper material properties and study. For the exact evaluation of losses, the Component wise study can be performed in the different setup of 2D model and the parameters can be closely studied. The main idea behind implementing this equation is to get an estimated theoretical idea of the hysteresis losses in the transformer core.

2.3 Magnetic Shunt

The usage of magnetic shunt is the main aspect of this thesis work. The main idea is to increase the leakage inductance of the transformer. To increase the leakage inductance of the transformer, the air gap between the wound primary and secondary windings is increased. This makes the transformer windings imperfectly coupled. The shunt core that is adjacent to the main core, acts like a gapped core inductor that acts like a inductance to the supply voltage by the primary.

Since the air gaps cannot be introduced in the main core, an additional shunt core is used that behaves like an inductor and stablizes the primary flux from sudden changes. This inductor also exhibits its own losses since it has air gaps that impact is its effective permeability.

For the effective inductance, the air gap could have been one big air gap at each leg. but due to this , the system would experience fringing effect flux. To mitigate this, the air gaps are distributed at constant lengths and finally as a whole represent a single air gap that would have been otherwise used as a single air gap. This helps in saving the flux from distortion.

The implementation of the inductance in the output of the inverter or input to the transformer as a filter is quite important for the power quality.

3

Methods

COMSOL Multiphysics is a simulation software that uses numerical methods for the solution of model. The software simulation is performed by using a combination of specified physics for a more realistic approach of the real life phenomena. The model is built from the basic level of geometry, application of the type of study is performed and modifications of the parameters for the types of postprocess required are carried out.

For this modelling, The AC / DC Module of the COMSOL Multiphysics is used that is an add on package for simulating the electromagnetics phenomenon on the model. In this section, highlights on the modelling stages and useful points from the AC/DC module are gone through.

3.1 Geometry

There are several primitive shapes inbuilt in the software which makes it quite user friendly to implement. In cases where a user defined shape type is required, the shapes can be built by multiple operations that gives full flexibility to an extent of making complicated designs.

For each design shape, a basic primitive geometry is used to make the base design. The design is then operated using geometry operations including boolean operation and transformation operations. For the objects that are adjacent to each other or overlapping, there are operations like forming union or forming difference or assembly.

The geometry is made from the scratch starting with a plane. As the model is a 3D model, Each plane for a particular part has a separate plane geometry. After making a top view of every particular component, the part is extruded out in the direction in which it is supposed to form as normal.

3.1.1 Core

Work plane 1

Model building is started with making the geometry for the core first. A plane with the desired shape is cutout in the X-Z direction. After performing operations, the core comes out in 3D as:

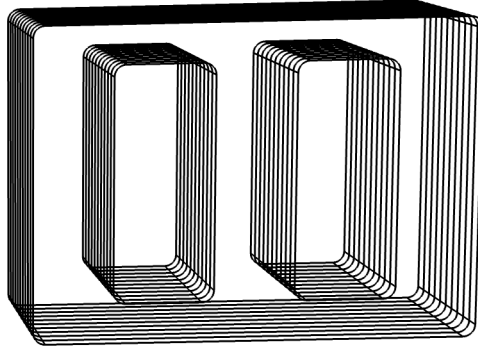


Figure 3.1: Core for the transformer model

To keep the report concise , the geometrical steps that are taken are mentioned with figures in appendix.

For the core,the exact thickness of the laminations stacked together couldn't be made as it is complicated for the solver and implement the lamination stack for thickness of 0.5 or 0.3 mm or the specified length.However an approach to realise it by properties is mentioned in the sections followed.

3.1.2 Shunt Core

Work plane 4

The plane for the shunt core was cut out at a distance, after the main core was extruded according to the dimension. From the main core in X-Z direction and extruded outwards in the -Y direction of the coordinate geometry.

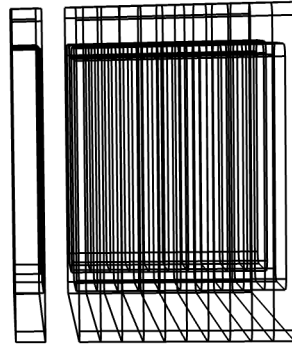


Figure 3.2: Shunt core and main core

The following figure is the view of the shunt core. This is built inclusive of all the air gaps, that gives it a property of the inductor. It contains a total of 13 air gaps in each leg.

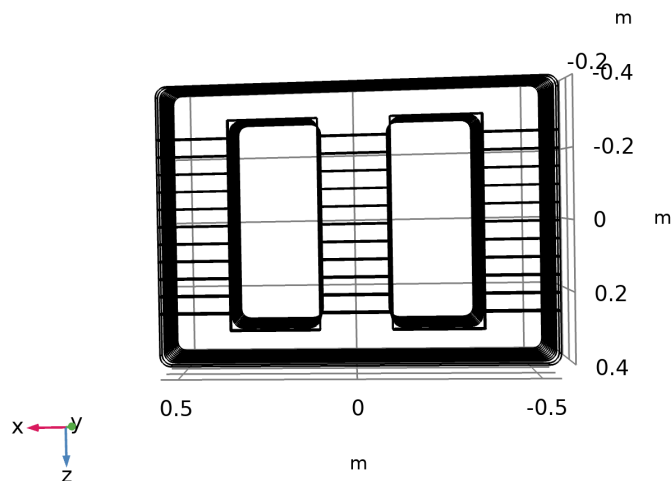


Figure 3.3: Air gaps present on shunt core

These air gaps are at a constant distance from each other throughout the length of leg of shunt core. The dimensions of air gaps are:

Table 3.1: Air gaps

Number of Air gap	length of air gap(mm)	Located
2	0.5	One at each end
11	2	Centre and equidistant

3.1.3 Windings

Work plane 2

for the windings, the XY plane is cut out in the shape geometry for both windings. It's position is then adjusted within already constructed core and shunt core. same as the above cases, this XY plane is extruded in Z direction.

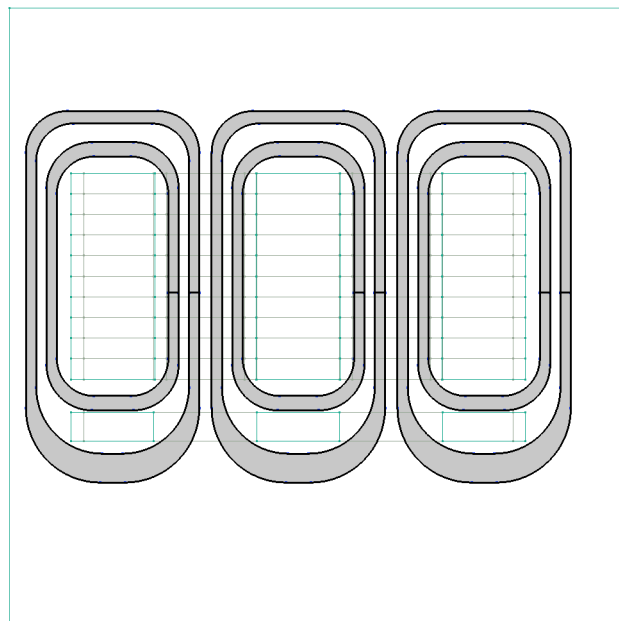


Figure 3.4: Winding plane geometry

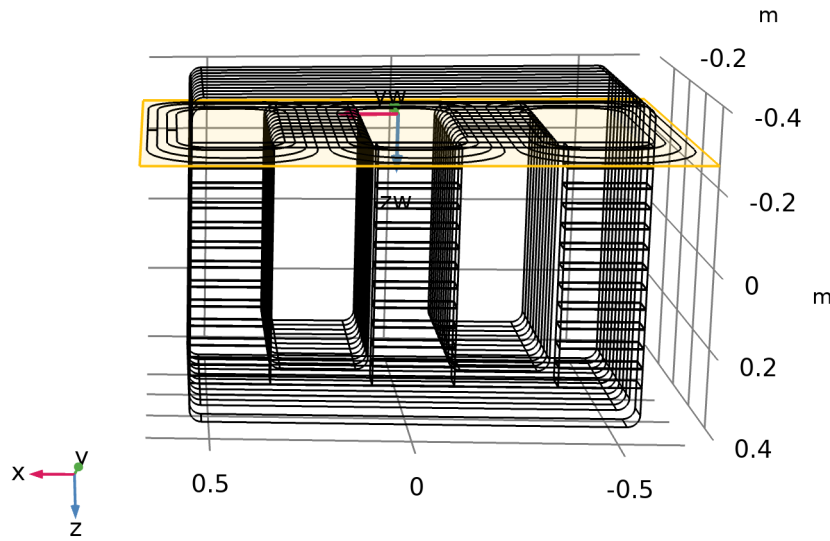


Figure 3.5: Winding geometry process

Finally after completing the geometry steps, a full model of the transformer is constructed. This model doesn't include the carpentry and external casing.

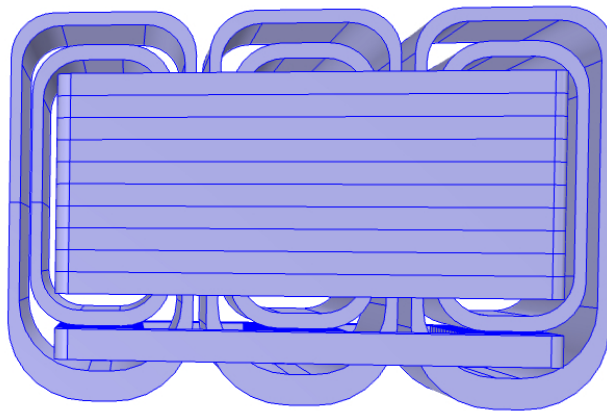


Figure 3.6: Complete model top view

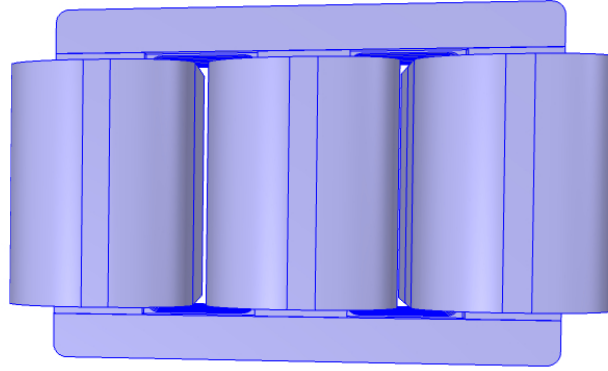


Figure 3.7: Complete model front view

The materials are assigned to the domains made, but just outside the model there is no medium set. This model is enclosed in a cube having the medium as air in order to behave like a normal transformer. The modelling of carpentry and casing of the transformer is not included in this transformer model.

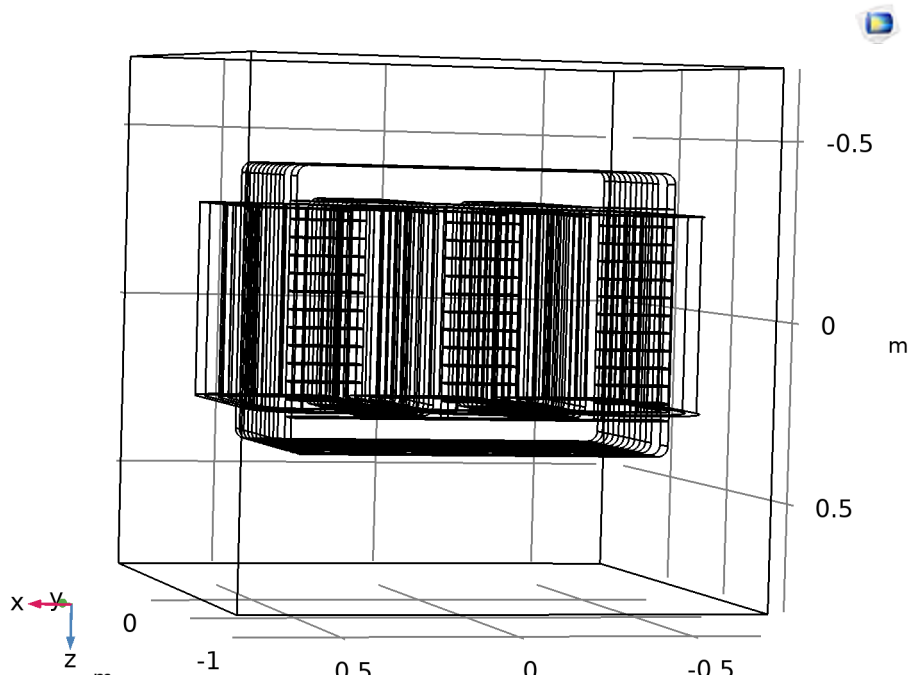


Figure 3.8: Full model

3.2 Materials

A suitable material is the absolute requirement for the devices working on the principle of electromagnetic induction.

Material Contents					
Property	Variable	Value	Unit	Property group	
<input checked="" type="checkbox"/> Electrical conductivity	{sigm...	{500[S/...	S/m	Basic	
<input checked="" type="checkbox"/> Relative permittivity	epsilo...	1[1]	1	Basic	
<input checked="" type="checkbox"/> Relative permeability	mur_is...	8500	1	Basic	
<input checked="" type="checkbox"/> Heat capacity at constant pres...	Cp	812	J/(kg·K)	Basic	
<input checked="" type="checkbox"/> Density	rho	6000	kg/m ³	Basic	
<input checked="" type="checkbox"/> Thermal conductivity	k_iso ;...	34	W/(m·K)	Basic	
Magnetic flux density norm	normB	BH(nor...	T	B-H curve	
Magnetic field norm	normH	BH_inv(...	A/m	B-H curve	
Magnetic coenergy density	Wpm	BH_pri...	J/m ³	B-H curve	

Figure 3.9: Material properties

For time dependent and stationary studies, the BH curve is used in COMSOL. This BH curve is not useable directly in frequency-domain studies. The use of this effective BH curve approximates the behaviour of magnetic materials that are non linear , in frequency domain simulations. Using this effective BH curve, the approximate response of the material to a time domain excitation is computed, without the same computational time and cost.

For solving the problem in frequency domain, an average of the properties over a cycle is considered. This averaged curve approximates a non linear material at the fundamental frequency.

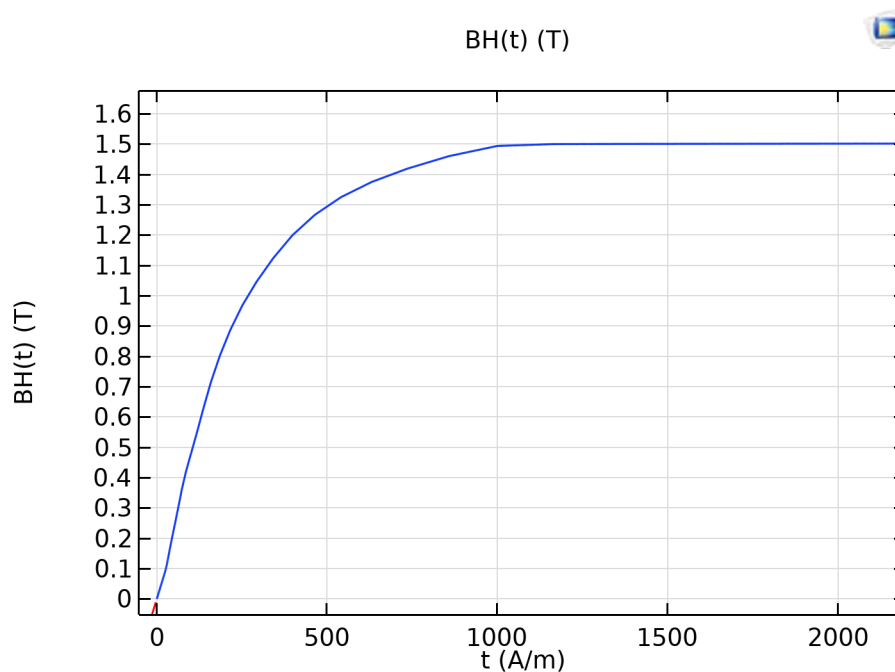


Figure 3.10: BH Curve for Silicon steel GO

The Figure represent the averaged BH curve for the chosen material for the computation. As inferred from the curve, the hysteresis is not considered for this material. The material saturation is at around 1.5 Tesla. This material BH curve is applicable for the time domain simulations performed.

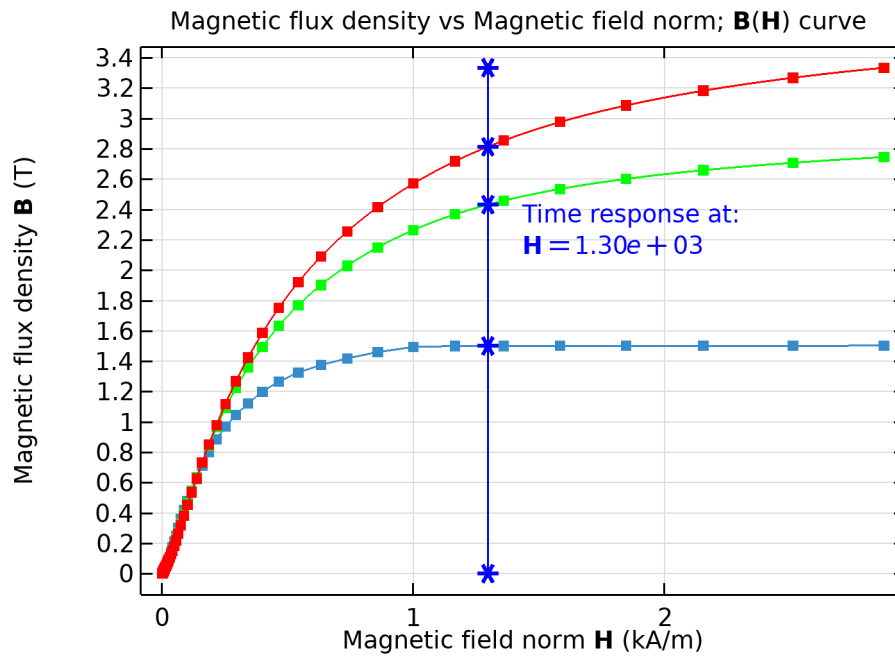


Figure 3.11: Effective BH Curve for Silicon steel GO for frequency domain study

The effective BH curve is the one that is used for the frequency domain simulations in this system. It approximates the behaviour of a nonlinear core in the frequency domain application. The Two equivalent curves of Average Energy and Simple energy are computed from the existing BH curve of the material by the help of an application provided by COMSOL. The green plotted line represents the approximation by using simple energy approach and the red one is using the average energy approach for the approximation.

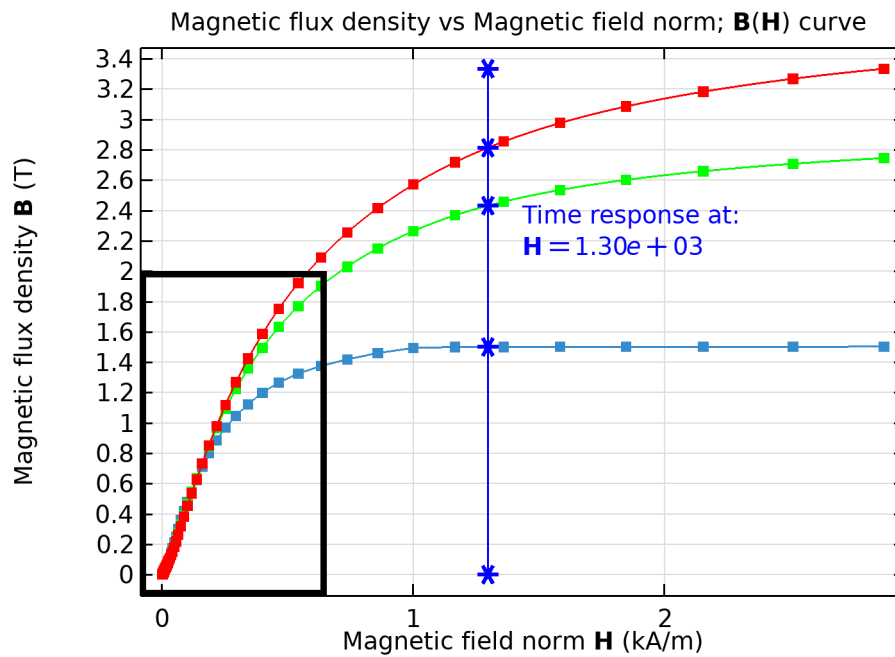


Figure 3.12: Range for Effective BH Curve for Silicon steel GO for frequency domain study

The curves reaching a high value of around 2.8 Tesla and 3.4 looks beyond the imagined value. More emphasis has not been given to this as the range of study is as marked in the figure, at which the operational range is understandable.

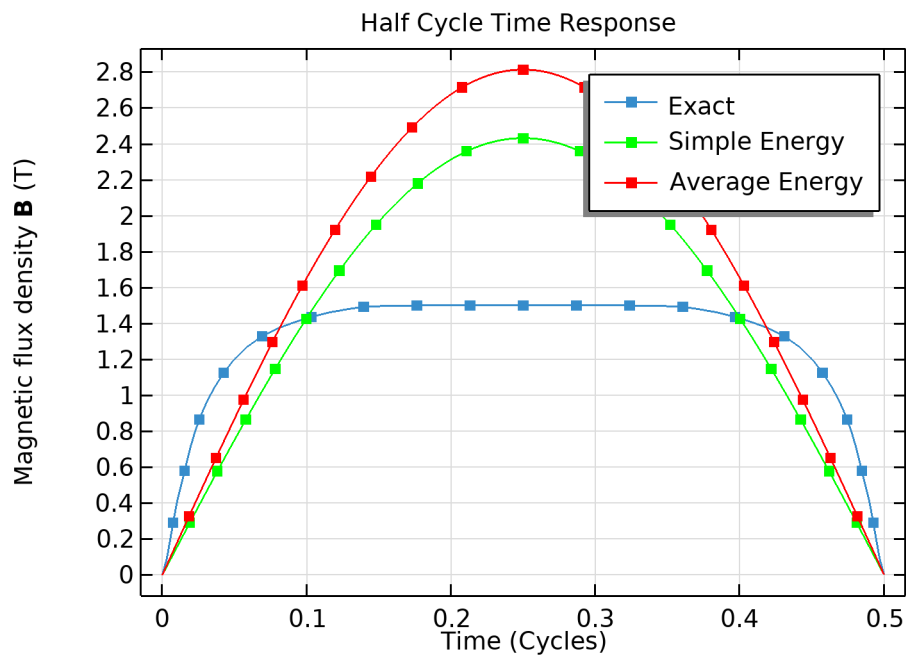


Figure 3.13: Cycled average for half time cycle

This Averaging is done by two inbuilt methods:

$$B_{SE} = \frac{2}{H} \int_0^H B(H) dH$$

$$B_{AE} = \frac{16}{TH} \int_0^{T/4} \int_{H(0)}^{H(t)} B(H) dH dT$$

where,

H - Amplitude of time harmonic magnetic field

B(H)- Material's non linear relation

H(t)- Time dependent oscillating magnetic field

T- period of oscillations

ref-[15]

An in-depth analysis of these calculation is not performed as there is an application that can compute the effective BH curve of a material by using the extrapolation data of the normal BH curve of the material.ref-[22]

When a BH curve of a magnetic material is plotted by data from testing , there might be unusual spikes and deviation from a well plotted curve due to errors in measurement. This can be a problem in the computation of a model if a BH curve from the actual material used has to be applied and sometimes can even lead to a non converged solution. During such events,an algorithm defined in one of the application can be used that optimizes the uneven deviations in the plotted curve considering the physical aspects.

3.3 Mesh

The finite element subdivides the model into smaller domain called elements over which the equations are solved. The meshing of the model defines how accurately the geometry is solved.Four element of different types are used to define the mesh of the created geometry.These include the following shapes- terahedron, pyramids, triangles and hexahedrons.After choosing the desired shape , for a better computation the size of the selected element can also be changed to the preset sizes available in the software.The element size can be set in several steps ranging from extremely coarse to extremely fine.

For the simplicity and quick solution of the model, free tetrahedral shape is set to the meshing sequence of this model. The size of the elements is kept coarse. For the primary solution the size of the refinement of elements is considered coarse so that the time for evaluation of the model is less. Also the mesh refinement for a fine case would be computationally demanding , so fo the estimation of parameters simple meshing sequence was preferred.For a more clear estimation of parameters and accuracy, the elements size could be refined.

Referring to the statistics of the mesh sequence, the geometry contains a total of 170921 elements.These elements cover the volume area of 3.375 m³.

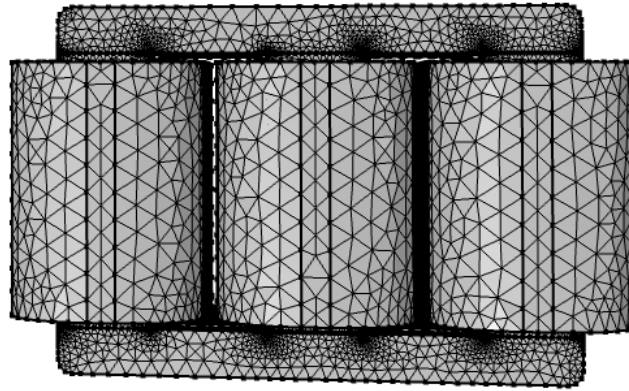


Figure 3.14: Mesh for the model

3.4 Magnetic fields

The magnetic field interface is the physics for the setup of the model. It solves Maxwell's equations by using magnetic vector potential. This interface computes induced currents and magnetic field inside and around the conductors and the model as whole.

This physics works, based on the equations:

$$B = \nabla \times A$$

$$\nabla \times H = J$$

$$n \times A = 0$$

The Ampere's law node uses the equation :

$$\nabla \times H = J$$

where,

H- Magnetic field intensity

J- Current density

This means , the curl of the magnetic field intensity at a point is equal to the volume current density at that point.

The equation is derived from the equation of Ampere's circuital law:

$$\oint H \cdot dl = I_{enc}$$

By using Stoke's theorem - 'The line integral of vector field over a loop is equal to the flux of its curl through the enclosed surface'

$$\oint_c H \cdot dl = \int_s \nabla \times H$$

I_{enc} can be expressed as:

$$I_{enc} = \int_s J \cdot ds$$

combining the equations we get,

$$\int_s \nabla \times H = \int_s J \cdot ds$$

Therefore,

$$\nabla \times H = J$$

3.4.1 Coils

For the model, the windings are implemented using the coil subfeature under the magnetic field interface. The coil feature is used to set up the winding geometry in the model. Specified number of turns of primary and secondary winding is entered. For the ease of remembering the coil is given a numeric value, which also helps in categorising the coil as primary or secondary.

For the more realistic replication of the physical unit, the coils are chosen to be homogenised multi turn with the chosen diameter and value of electrical conductivity. the mode of excitation for these coils is from the circuit current. The coils in the electric circuit interface are coupled to respective coils on primary and secondary. The electric circuit is computed and the resulting parameters are used to run the model. Since the physical coils have an insulation around the conductor the effective fill factor of the coils is reduced due to it. In this modelling , the fill factor of the coil including the insulation was not taken into effect.

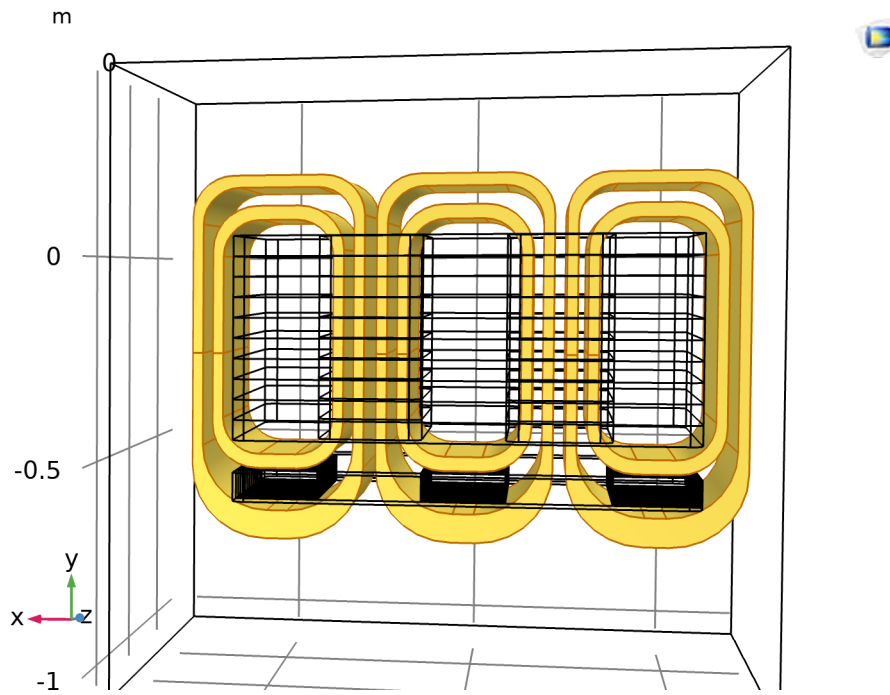


Figure 3.15: Windings of the transformer model

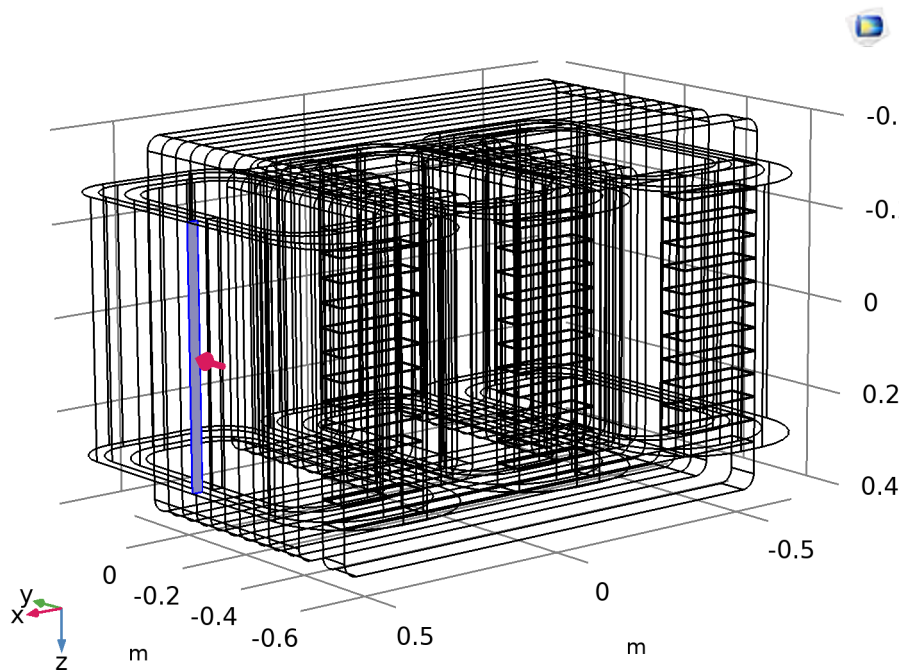


Figure 3.16: direction of input current in the coil

To replicate the polarity of the transformer, the direction of the current in the windings is specified as seen in the figure above.

3.4.1.1 Primary Windings

The coil numbers 1,2,3 are the primary windings. The primary windings enclose the main core and the shunt core . .

Ref Appendix

3.4.1.2 Secondary Windings

Coil number 4,5,6 are the secondary windings and only enclose the main core of the transformer model.

For each phase ABC , the pair of coils is

- Phase A - [1,4]
- Phase B - [2,5]
- Phase C - [3,6]

3.5 Electric circuit

Generally transformer are operated with Delta-Wye configuration for industrial applications. The delta connection provides a path to flow for the third harmonic component and so its not passed to the secondary side.

With the Electric circuit interface, the circuit is implemented to the model. The connections for the transformer are Delta for primary and wye for secondary windings. To interface 'Magnetic fields' physics with 'Electric circuits' interface the major nodal component used is the 'External I vs. U' .It connects a voltage measurement as a voltage source between two nodes in the electrical circuit. The circuit current between the two specified nodes is coupled back as current source in form of voltage measurement.

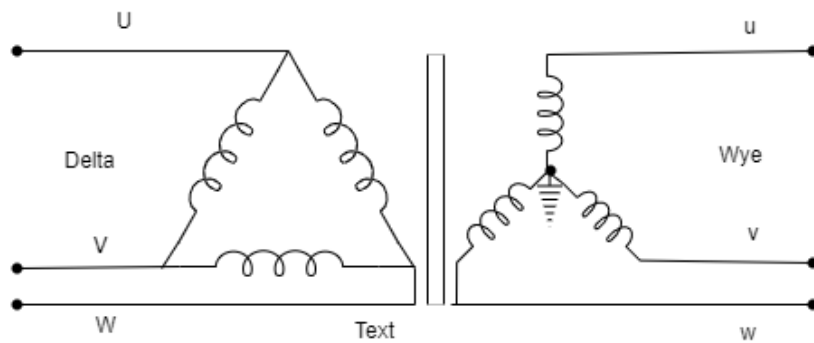


Figure 3.17: DY connection

The following figure shows that exact implementation of windings in the model. The coils represent the 'External I vs U' component. A small resistance needs to be added parallel to the coil to make it run, otherwise an error in the structural consistency occurs in the model. These resistance however do not effect the results.

In the Delta side, each source represents a particular phase voltage U,V and W. To reproduce the exact physical system these phases have an phase angle of 120 degrees

or 2.0944 radians. However in reality, the incoming voltage from the inverters is not perfectly sinusoidal due to the PWM switching as it contains the ripple patterns. An assumption is made here that the minor ripples doesn't have much effect on the losses of transformer and studying it with the normal sinusoidal option can be used. On the wye side, the centre of the circuit i.e the neutral is grounded. Both the ground nodes are unique and isolated from each other. These coils are coupled as windings in the magnetic interface.

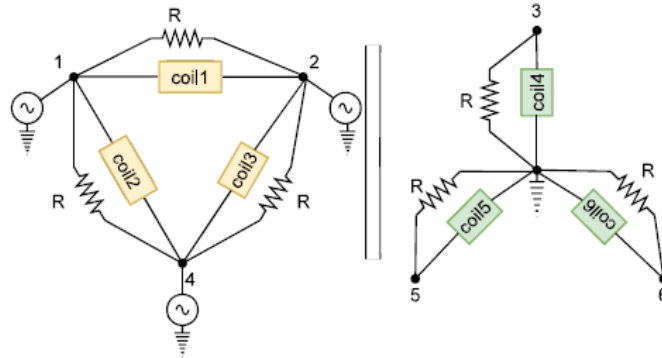


Figure 3.18: Electrical circuit as in model.

To simulate the effect of filter capacitance for further work, the capacitors are connected to the output secondary side of the transformer in Delta configuration. An analysis on the values for the open circuit test with Delta connected capacitors was done, but it is not included in the results.

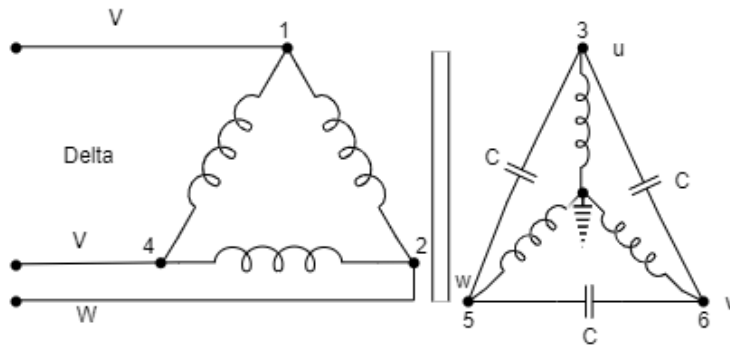


Figure 3.19: Electrical circuit with filter capacitance.

3.6 Study

At this level, the model is set with its geometry and the properties. The final processing for solving the model for the implemented physics is performed in this step. The results of the variables for the This sections consists of the steps and methods used to compute the model. Two study steps are used for the study.

First is coil geometry analysis. this analysis is used to compute the current that flows in the defined coil features in the 3D models. This step is the base step when coils are used and its a pre processing step that has to be solved before main study can be computed.

For the model the coil type is numeric so for each coil number the parameters are solved and specific direction of current flow in the coil is provided beforehand by the user.

After analysing the coil geometry , the frequency domain study is set. This study and its steps compute the effects of frequency when applied to the linearized model.

4

Results

A successful simulation study is run on the developed 3D model of the 3 phase transformer. The simulation results are analysed by the post processing steps in the software, by the help of which certain plots are generated and the evaluation of the parameters is done.

The post processing steps include operations on the calculated variables of the model. Depending on the evaluation required, the computed variables are used in mathematical function which provide the values. The losses are calculated using the Volumetric loss density over the components and then integrating it over the domain of each component. This provides the value of total losses for a particular domain.

The Analysis is performed on the base frequency i.e 50Hz and then the harmonic frequencies as a result of the Pulse width modulated inverter output. The harmonic content present in the incoming voltage to the transformer was provided in the documents available for reference of this work. Along with the harmonic frequency, the voltage level was specified for the open circuit test and the current level was specified for the harmonic in the short circuit test.

The implementation of all the frequencies together could not be performed, rather a test case was simulated for every frequency at a specified voltage level or current, depending on the specifications. The results of the individual frequencies were then summed up for the final values.

The calculation of losses is done in two steps

- Open circuit test case
- short circuit test case

Assumptions were made for the calculations are specific to a particular test as its a model where some parameters needs to be adjusted.

For each testing case, the test is also performed with and without the shunt core present in the model. In order to perform this, the shunt core is replaced with the material as air resulting only main core active in the system.

In this section, the results of the open circuit test are plotted, following by the tabulated values of the losses with and without using the shunt core.

The similar analysis is done with the short circuit test for the model and the comparative analysis is done with the reference values available from the actual test on the physical transformer.

4.1 Open Circuit test

For the estimation of core losses of the transformer, the open circuit test is performed on the model. For this, rated voltage is supplied on the primary side of the transformer at a certain frequency while the secondary side of the circuit is made open circuit. The secondary coil in the model couldn't be made to behave exactly like in an open circuit rather a high resistance value was connected across the secondary windings. For the case, if the secondary winding was taken out of the electric circuit defined, the model did not solve due to interrelated components. To implement this a large resistance is set to a value of $[10^9] \text{ ohms}$

The resulting plots and figures for the open circuit test of the model while utilising shunt core are as follows:

1. The flux density pattern on the main core of the transformer model is seen on the figure. The maximum density on the core comes out to be 1.9 Tesla which can be seen limited to the edges and corners in the inside window of the transformer. The higher density at the top and bottom of the core maybe due to the dimension of the geometry, where the flux lines are densely populated. The flux can be said to be using shorter path, this could be normal in this specific transformer type due to the presence of additional core .

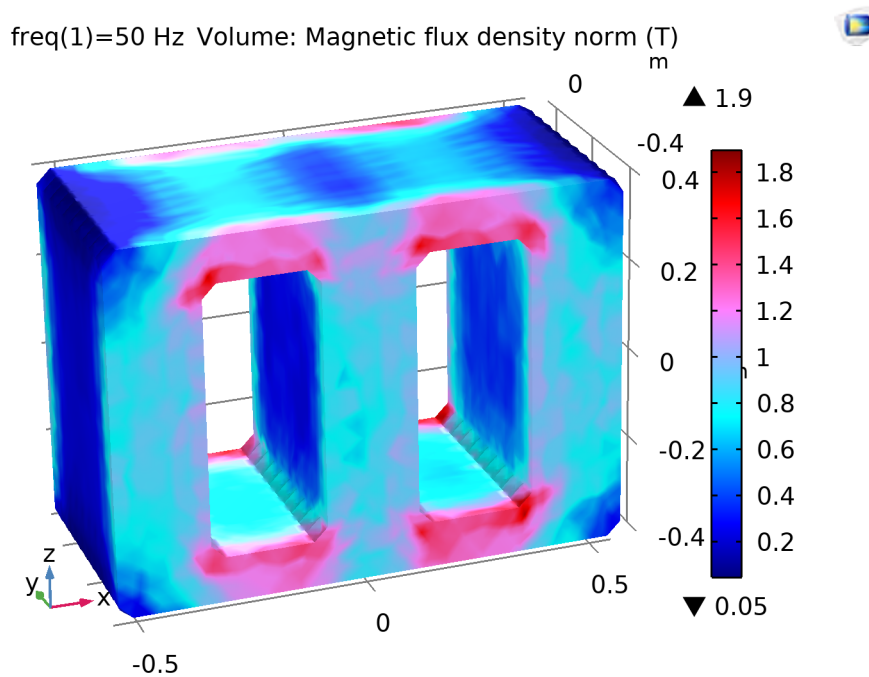


Figure 4.1: Magnetic field density on the main core

2. To observe the flux density in the interior of the core , the core was sliced in two components on the X and Z axis. The maximum field density can be seen on the extents of the core, majorly on the front and back edges of the core. The interior of the core seems to be fairly less magnetized than the ends. This uneven magnetization observed can be due to the value of conductivity of the material of the core. As expected, the flux density in the core is major in the interiors and reduced while

observed at the outer edges.

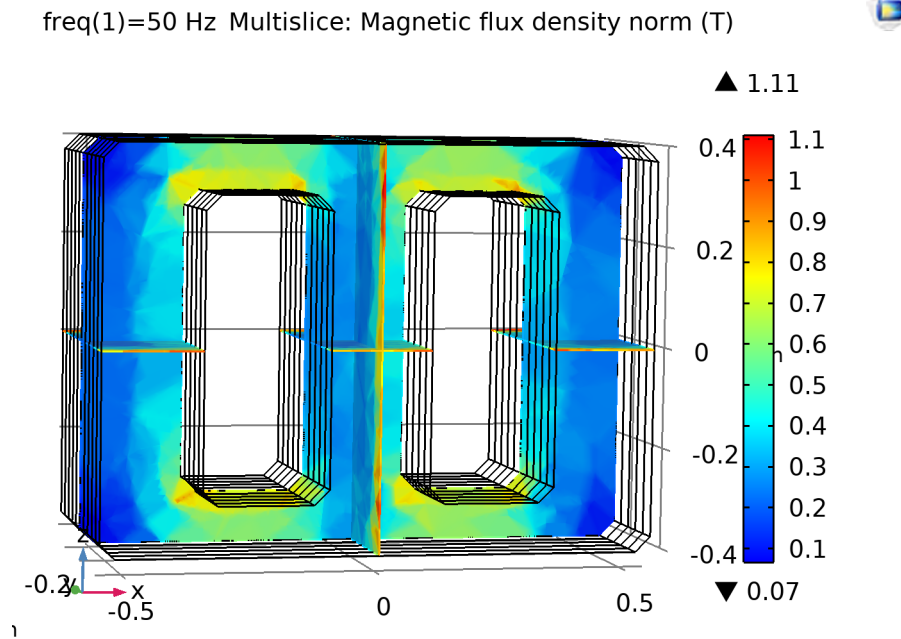


Figure 4.2: Magnetic field density mutlislice

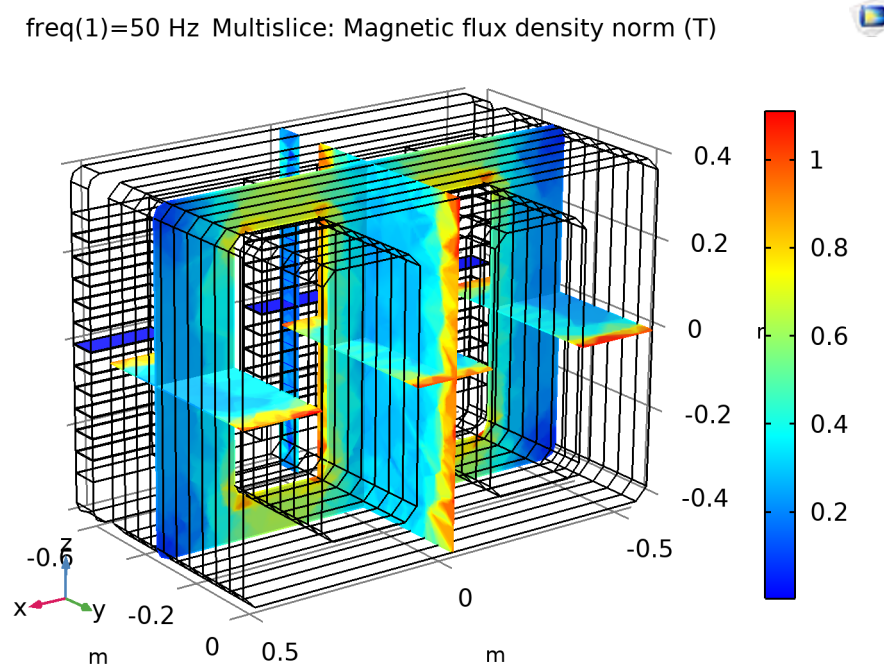


Figure 4.3: Magnetic field density multislice 2

3. The contour of magnetic field intensity is plotted on the figure , it shows the level of intensity mostly dense at the side legs of the transformer core which gets quite dense at the corners of the model.

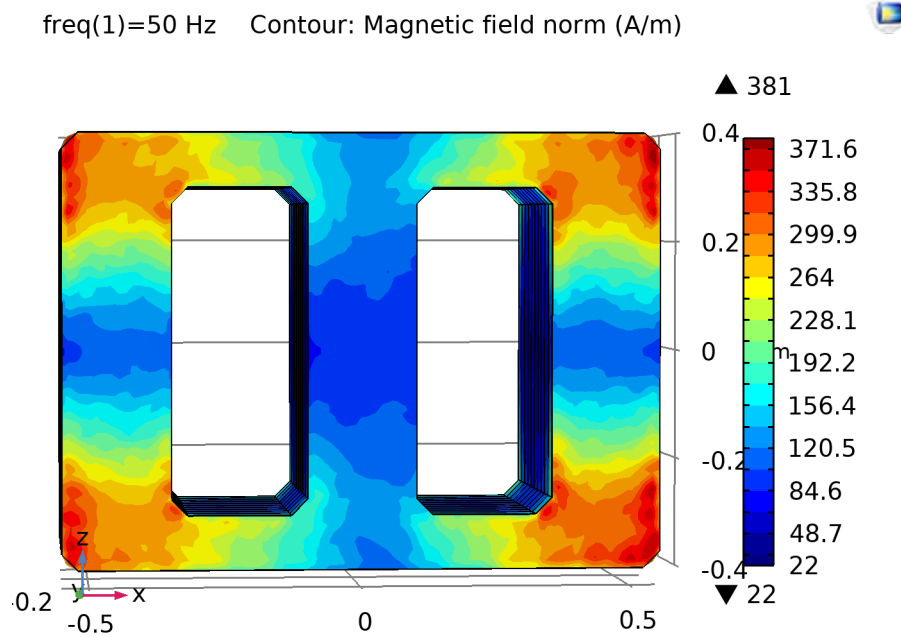


Figure 4.4: Magnetic field intensity

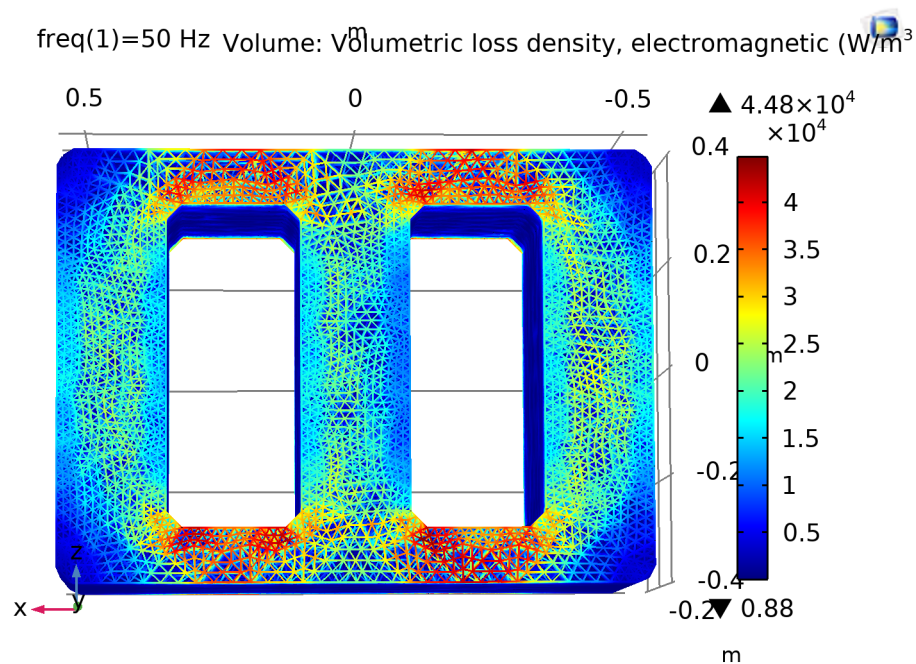


Figure 4.5: Loss density

4. The evaluation of the losses for the open circuit test is done by the total volumetric losses over the domain. For the observation of losses from the parts of the core the loss density of the core elements is plotted in the figure below, which represents the Finite elements losses. The maximum value of volumetric loss density on the

core is evaluated as $4.48 \times 10^4 \text{ W/m}^3$ similarly , the volumetric loss density from the top view of the core can be seen as:

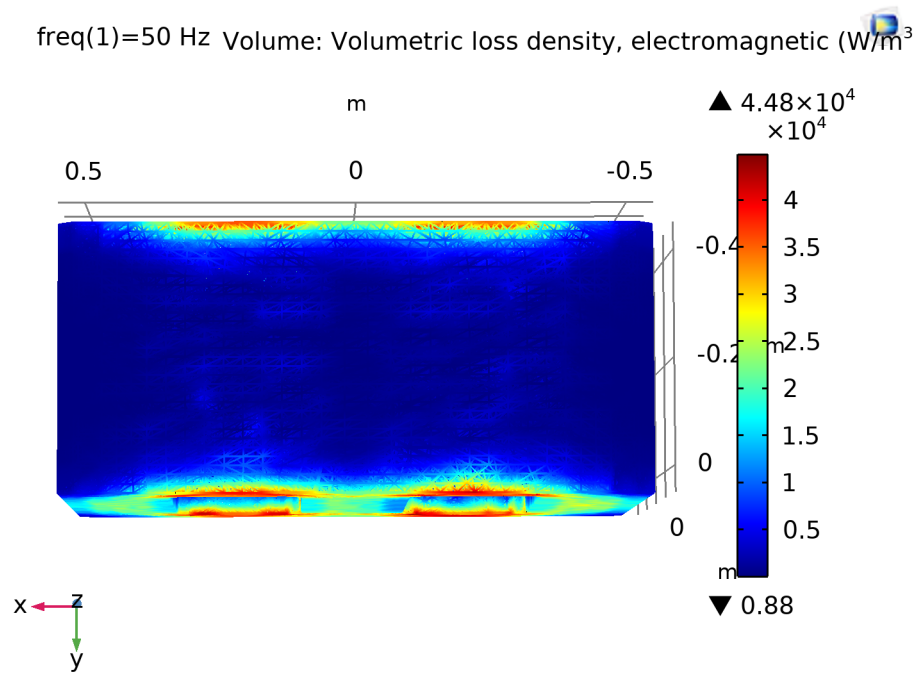


Figure 4.6: Loss density top view

5. There is a surrounding electric field due to the electromagnetic nature of the phenomenon that governs the transformer principle. The plot of the equipotential surface for the electric field is plotted for the model. A stronger field of value up until 20.29 V/m can be seen from the evaluated figure while the electric field value on the outside of the model is around 2.25 V/m . A stray Electric field around the electromagnetic device can be contained by using the electric conducting material as a shield outside.

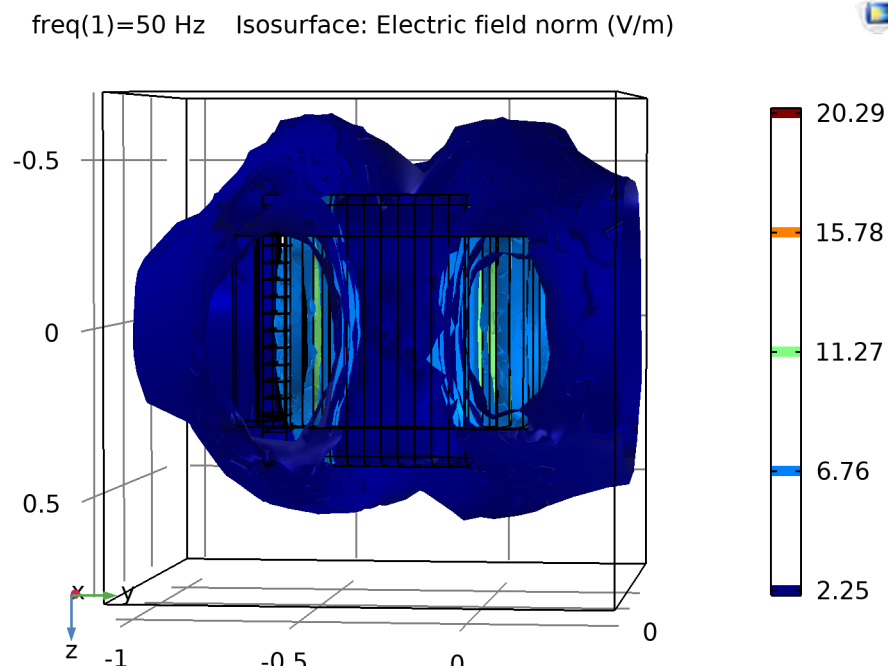


Figure 4.7: Electric field around the transformer

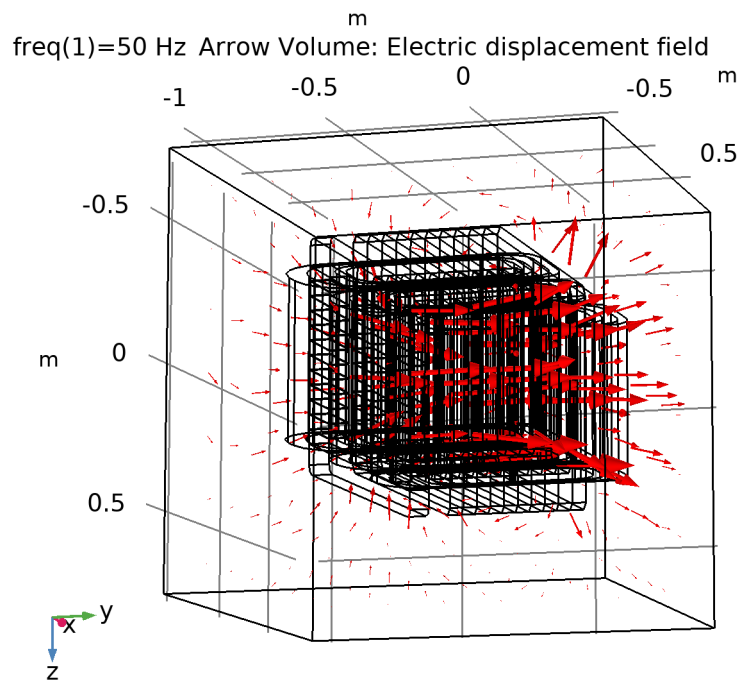


Figure 4.8: Electric displacement around the transformer

6. The magnetization plot of the transformer model is represented by the purple arrow cones in the figure. the magnetization field can be seen cycling in the two cyclic direction at a particular instant .

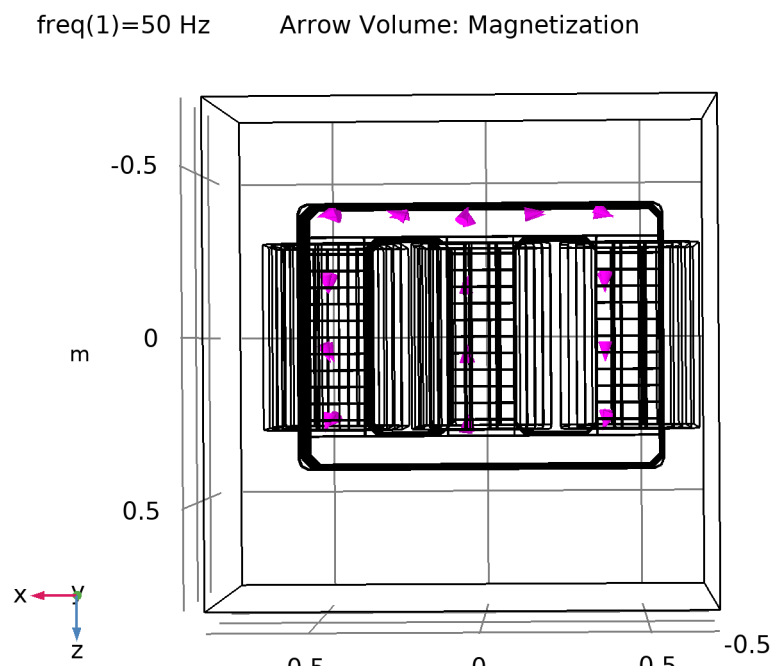


Figure 4.9: Magnetization in the transformer core

7. For the analysis of the shunt core , the plot of for the magnetic field density in the shunt core shows the distribution along the domain. The field seems to be highly dense in the top and bottom of the shunt core due to the dimensions and is reduced in the legs of the core probably due to the air gaps.

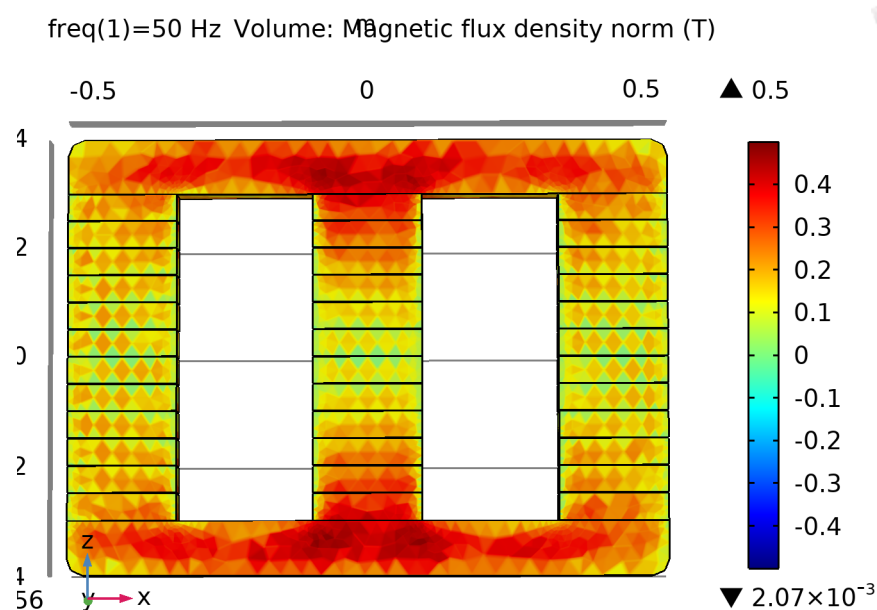


Figure 4.10: Flux density in the shunt core

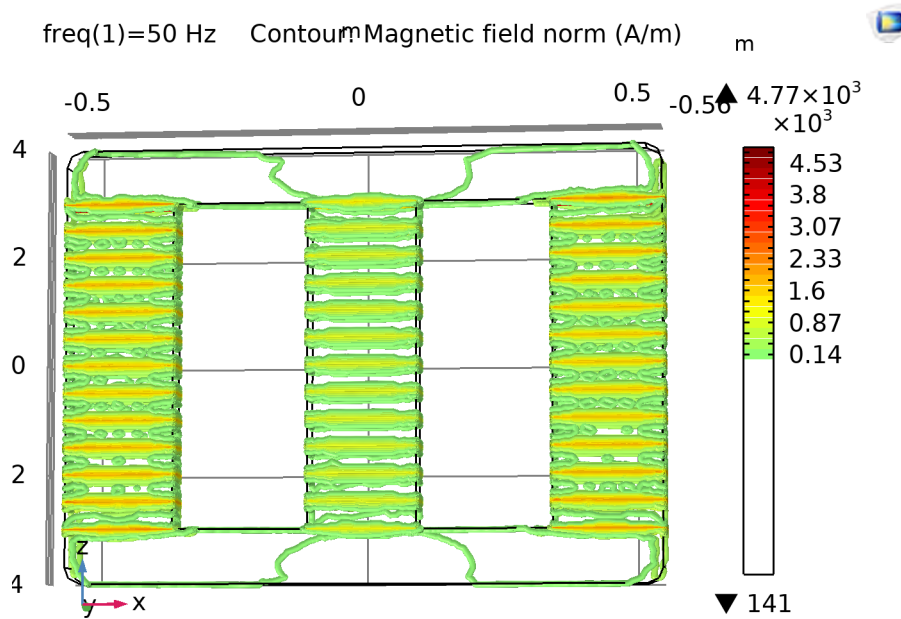


Figure 4.11: Magnetic field intensity in the shunt core

The effective value of magnetic flux density in the shunt core can be lower than in the main core due to presence of the air gaps (13 in each leg)

8. The volumetric loss density of the windings is plotted in the figure. At open circuit only the value of magnetisation current is drawn from the supply that comes out to be around 1.4 A in this model. The heat dissipated in the windings is only in the primary windings as no current passes through the secondary windings. the maximum loss density in the model is 1.5 W/m^3

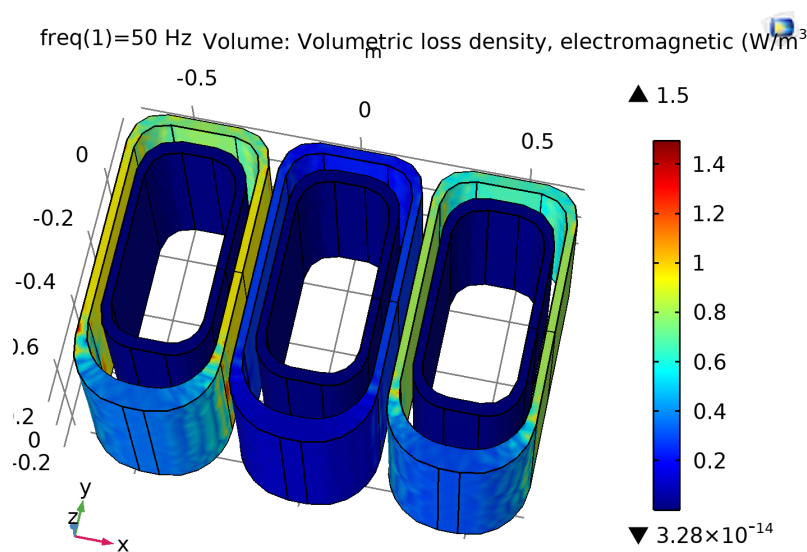


Figure 4.12: Loss density in the windings at open circuit

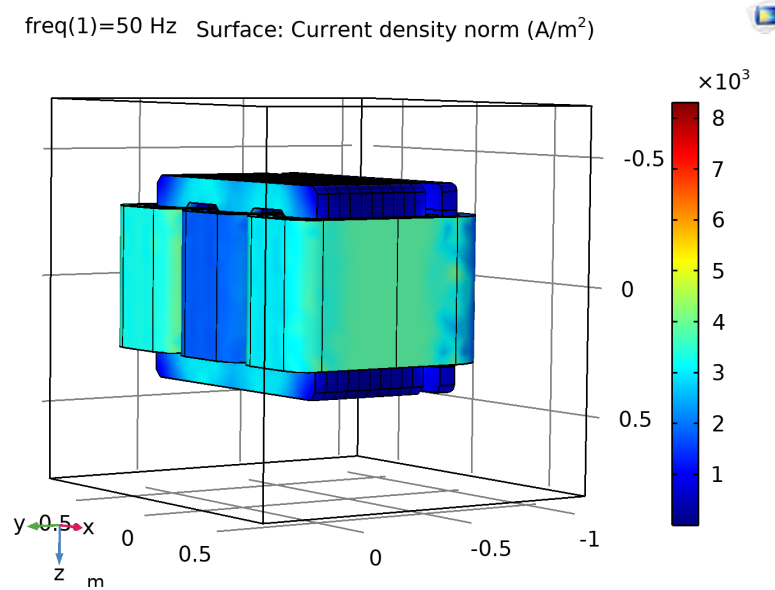


Figure 4.13: Surface load density in the transformer

4.2 Open circuit test with shunt core

The frequencies in the incoming line current to the transformer are taken from the reference description of the particular physical transformer. The model was simulated with the frequency described which are:

Table 4.1: Frequency based open circuit test

Frequency(Hz)	Voltage
50	650
3950	426
4050	422
5800	111
5900	152
6100	150
6200	101

Table 4.2: Frequency based open circuit test results

Frequency(Hz)	Steinmetz losses(W)	Main Core loss(W)	Copper loss(W)	Shunt core loss
50	476	787.63	0.0639	170
3950	6.97	132.83	0.0014	31.56
4050	6.66	129.91	0.0014	30.9
5800	0.31	8.5	8.8E-5	2.09
5900	0.57	15.9	1.6E-4	3.9
6100	0.54	15.3	1.59E-4	3.8
6200	0.24	6.95	7.1E-5	1.72

4.2.1 For all frequencies superimposed

The individual effect of the frequency listed in the table are evaluated on the simulation of the model. Keeping the approach simple, the result is summed up for all the frequencies.

The formula based expected hysteresis loss comes around 491 Watts. The main core losses for the open circuit test are evaluated to be around 1097 Watts and the losses in the shunt/inductor core are around 243 Watts.

Table 4.3: Cumulative effect of the frequencies

Steinmetz losses(W)	Main Core loss(W)	Shunt core loss(W)
491	1097	243.97

4.3 Open circuit test without shunt core

The model was run with the base frequency and the harmonic frequencies which are:

Table 4.4: Frequency based open circuit test

Frequency(Hz)	Voltage
50	650
3950	426
4050	422
5800	111
5900	152
6100	150
6200	101

Table 4.5: Frequency based open circuit test results without shunt core

Frequency(Hz)	Steinmetz losses(W)	Main Core loss(W)	Copper loss(W)	Shunt core loss
50	481.87	786.6	0.05	-
3950	7.4155	141.94	0.001	-
4050	7.1	132.2	0.0014	-
5800	0.349	9.53	6.8E-5	-
5900	0.643	17.875	1.2E-4	-
6100	0.6069	17.397	1.2E-4	-
6200	0.27	7.8847	5.6E-5	-

4.3.1 For all frequencies superimposed

Table 4.6: cumulative effect of the frequencies

Steinmetz losses(W)	Main Core loss(W)	Copper loss(W)
498.25	1113.42	0.05

4.3.2 Comparison of results with the physical test

Table 4.7: Loss Comparison to physical test results

Core loss from simulation	Core loss from physical test	Difference in Percentage
1340.97 Watts	1120 Watts	19.72 %

The difference in test results may seem to be quite much, but the physical test performed on the transformer model was done only on the base frequency, while for the simulation model we have cumulated the effect of base as well as harmonic frequency. Also the assumptions and simplicity of the model can be the reason for the value deviation.

4.4 Short circuit test

The short circuit test is carried out on the system for the estimation of copper/winding losses. The short circuit test is implemented on the model by applying a very low resistance across the secondary coils in the system. The rated current on the primary coils is applied based on which the losses in the system are evaluated.

1. The flux density pattern on the main core of the transformer model is seen on the figure. The maximum density on the core comes out to be 0.41 Tesla which can be seen limited to the inner edges and corners in the inside window of the transformers as well as on the front surface of the main core. The flux density in the corners of the core is stronger due to the non even distribution of flux [20] and may cause localised heating over it. The magnetic flux density in short circuit test is relatively lower than during the open circuit test as the secondary has exact opposite polarity of the load current in primary ,it therefore cancels out the flux that is created by each within the core. The color density is plotted for extremely fine element filter which brings about the density look like triangular elements.

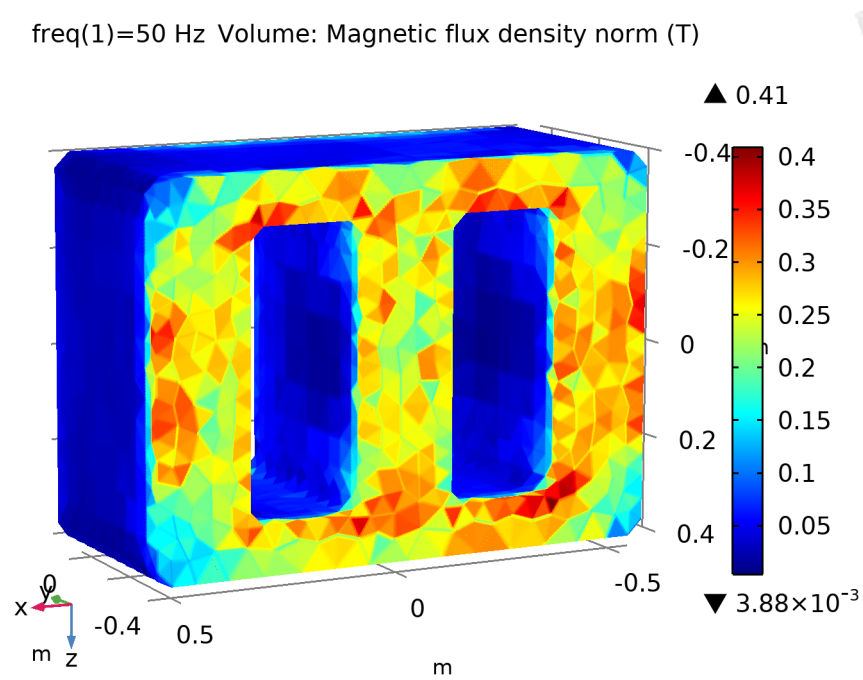


Figure 4.14: Flux density in the main core at short circuit test

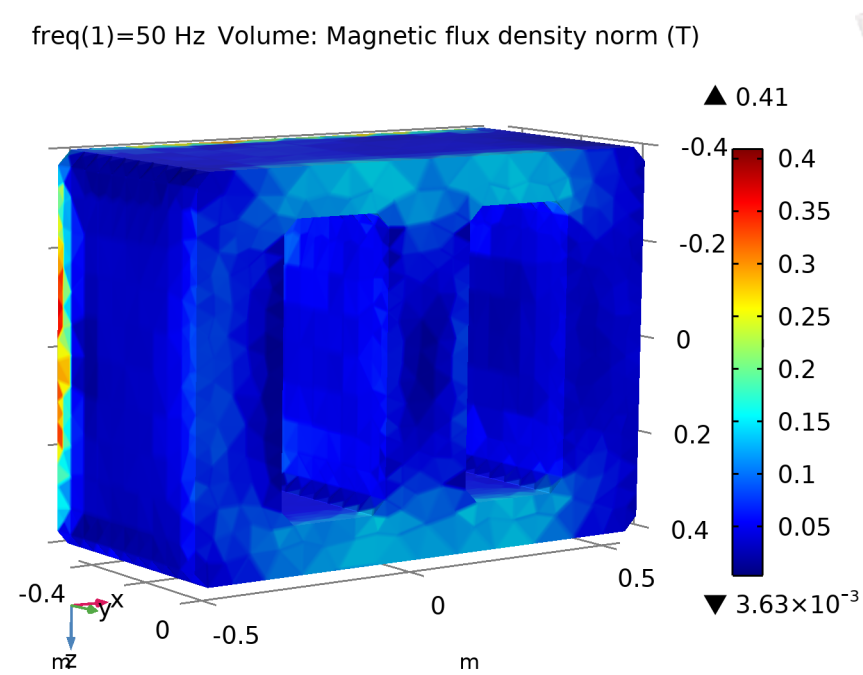


Figure 4.15: Flux density in the main core at short circuit test

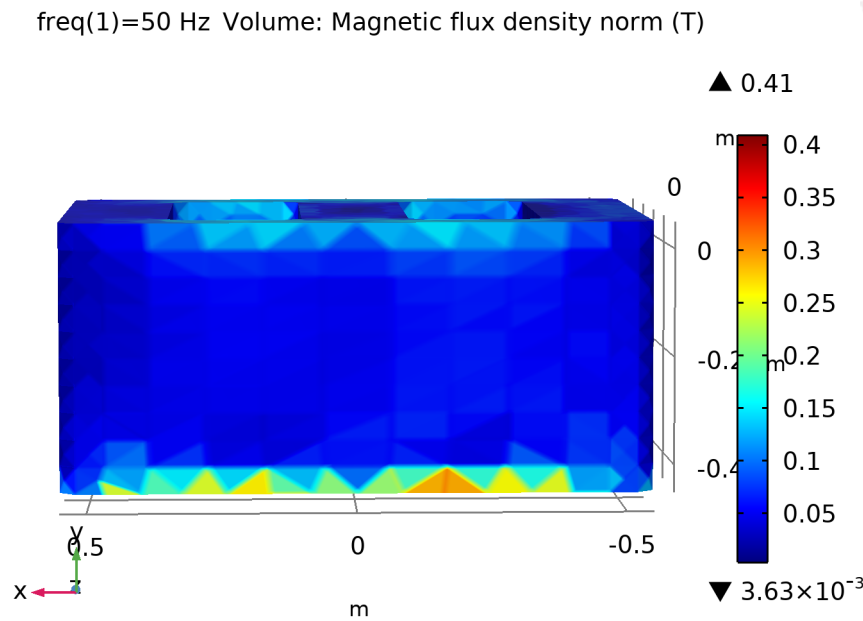


Figure 4.16: Flux density in the main core at short circuit test top view

2. The contour of magnetic field intensity is plotted on the figure , it shows the level of intensity mostly dense at the top and bottom of the the transformer core.

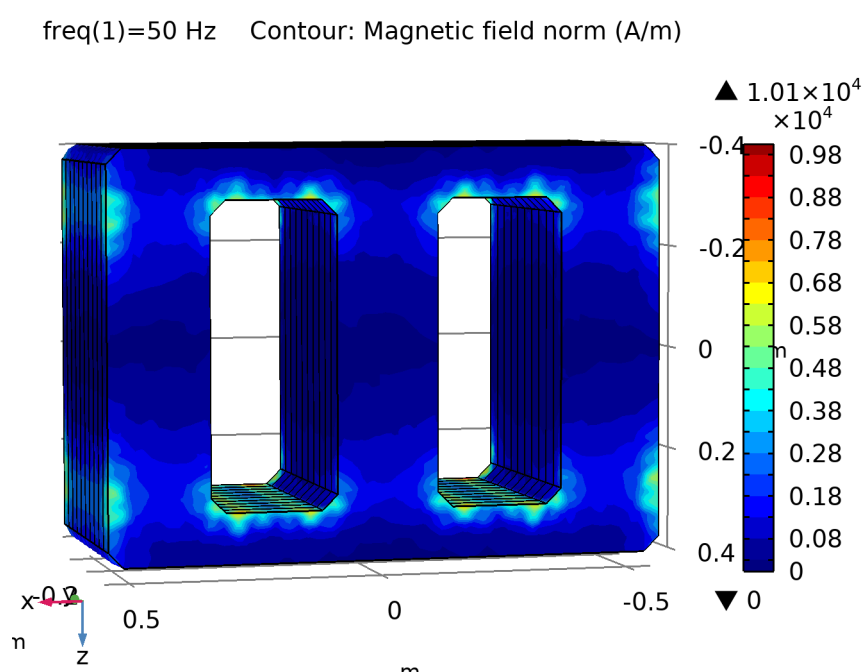


Figure 4.17: Magnetic field intensity in the core

3. The figure below shoos the finite element losses in the model.The loss density is more near the surfaces towards the windings . The maximum value of volumetric

4. Results

loss density on the core is evaluated as

$$6.07 \times 10^3 \text{ W/m}^3$$

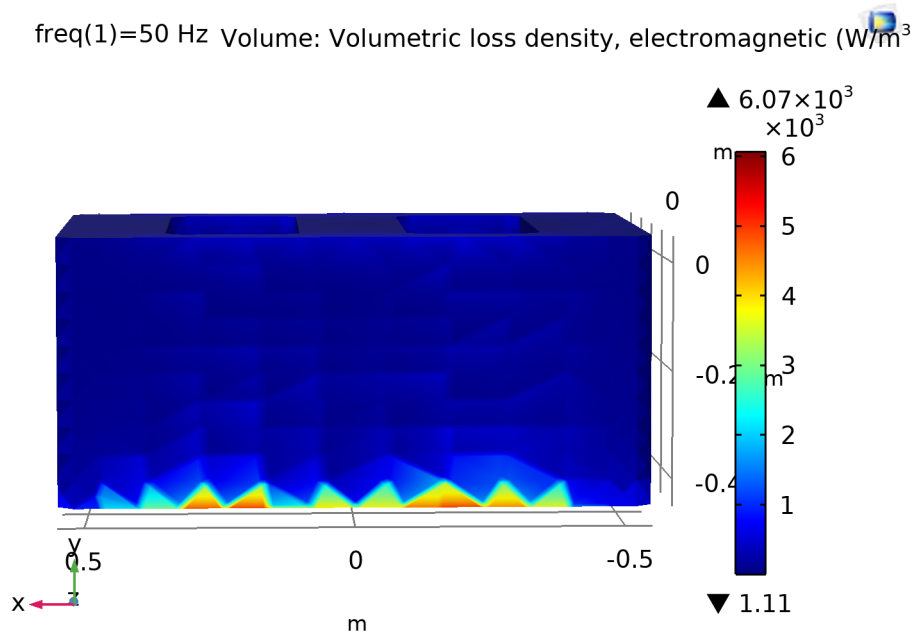


Figure 4.18: Loss density in the main core at short circuit test

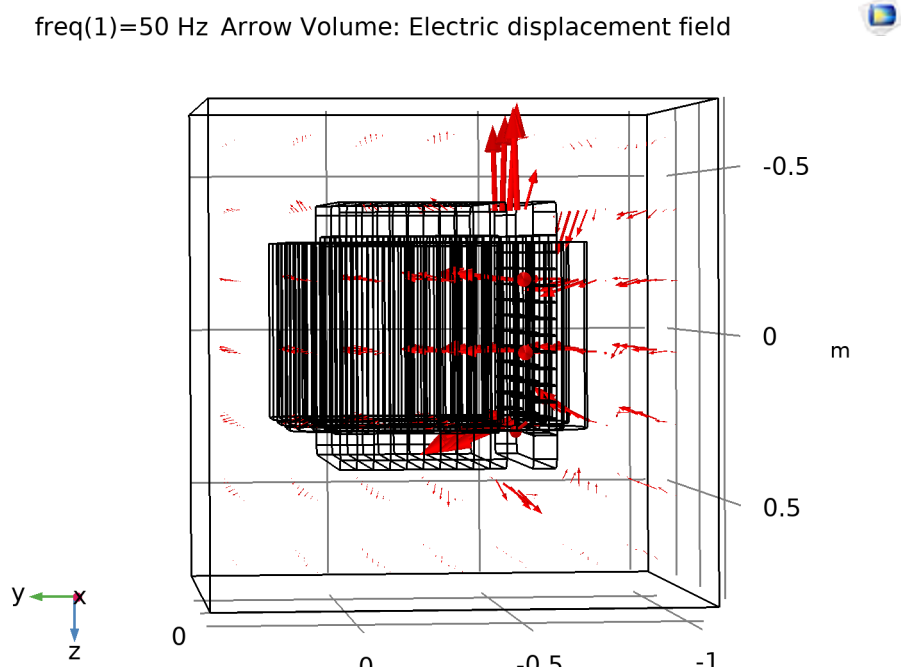


Figure 4.19: Electric displacement field

4. The plot of the equipotential surface for the electric field is plotted for the model. A stronger field of value up until 14.4 V/m can be seen from the evaluated figure while the electric field value on the outside of the model is around 1,6 V/m . A stray Electric field around the electromagnetic device can be contained by using the electric conducting material as a shield outside.

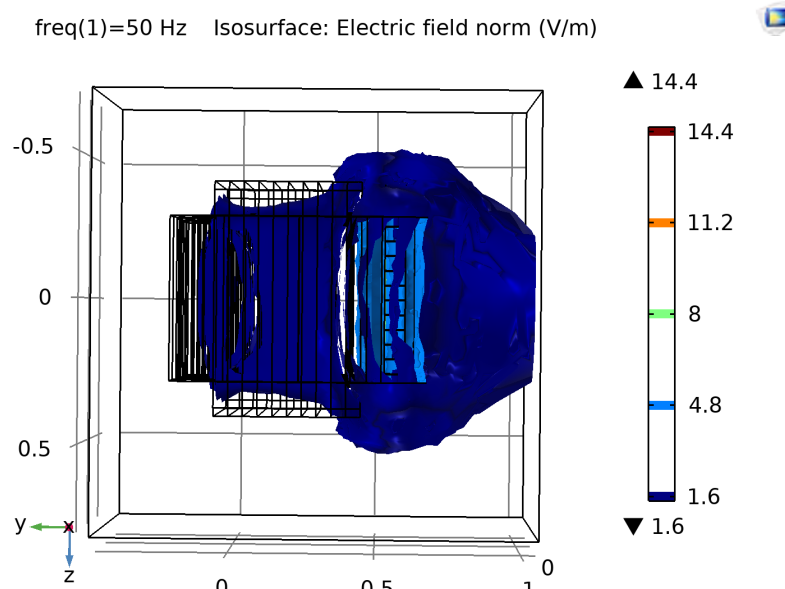


Figure 4.20: Electric field around the transformer during short circuit test

5. The surface plots for the magnetic flux density and volumetric loss density are plotted and it shows high flux density on the shunt core. As the flux on the shunt core is not linked to the secondary winding, it builds up and thus has a higher value.

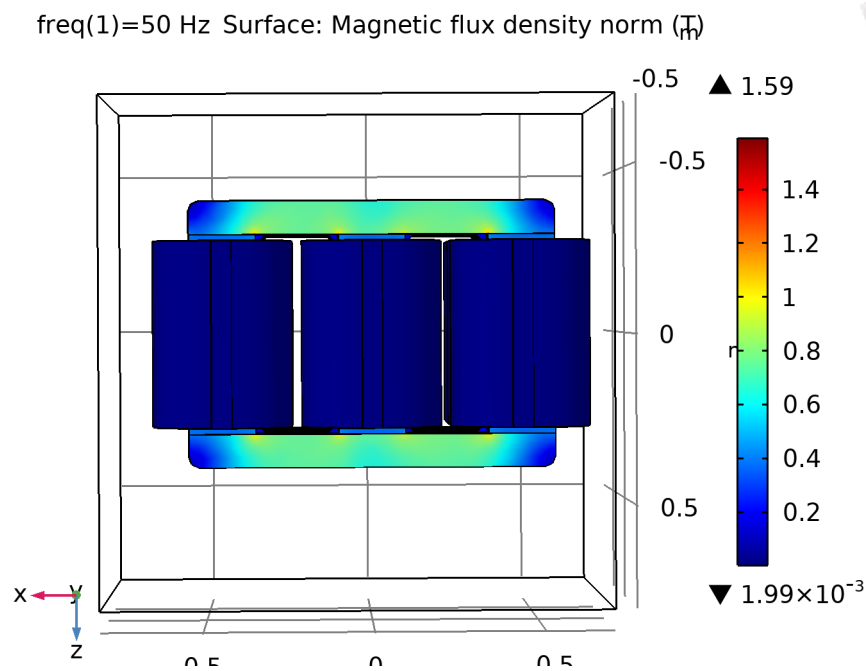


Figure 4.21: Magnetic field

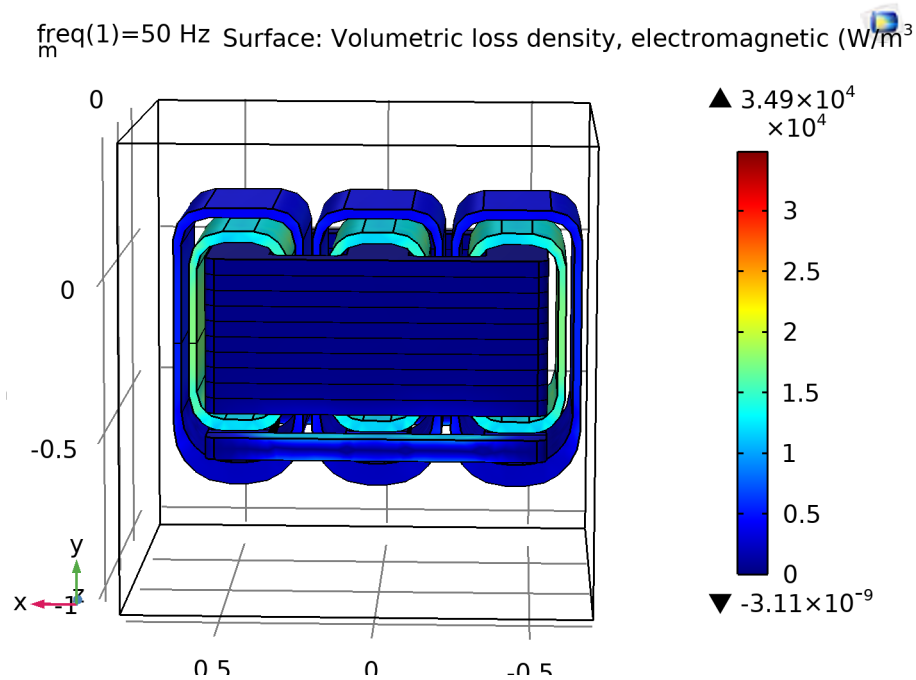


Figure 4.22: surface Volumetric loss density in the model

6. The plot for the volumetric loss density on the shunt core shows a relatively higher value. The ends of the shunt core legs have higher loss density as compared to the legs.

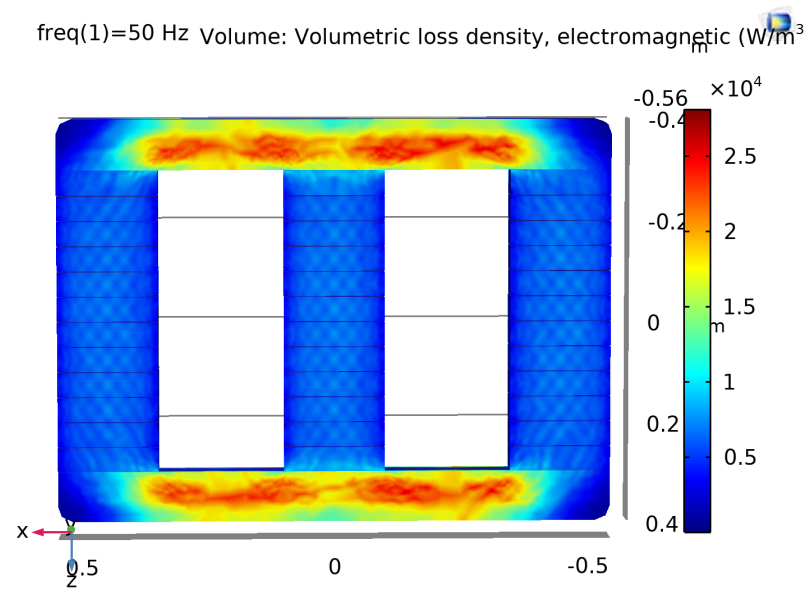


Figure 4.23: Volumetric loss density in the shunt core of the model

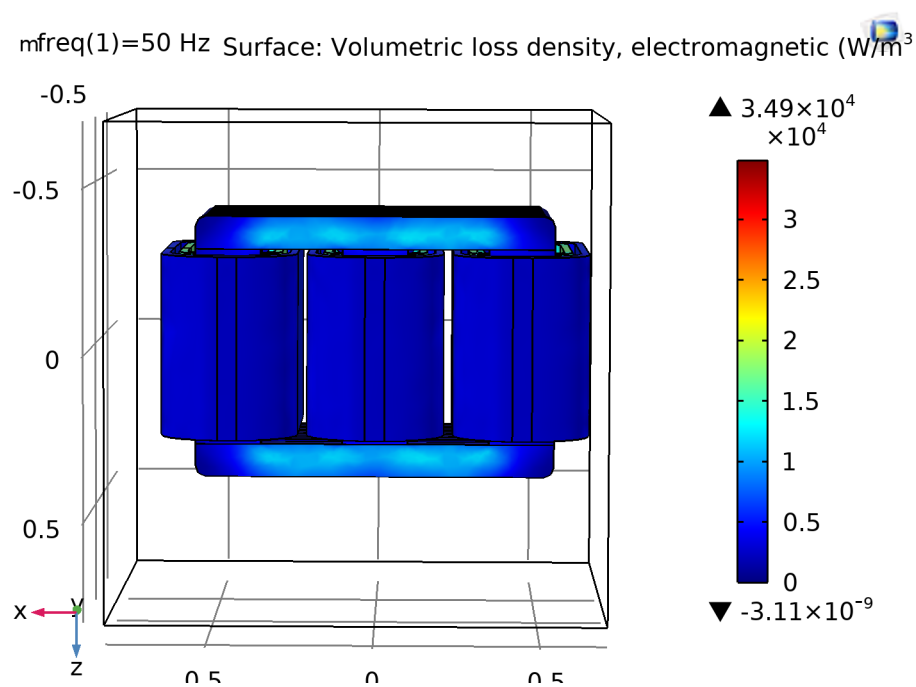


Figure 4.24: Volumetric loss density in the model view 2

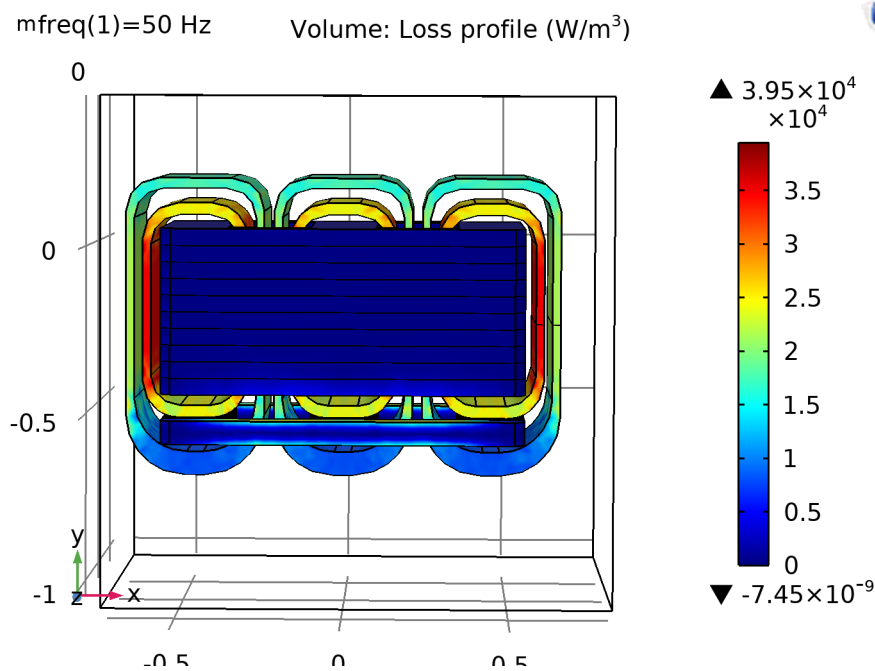


Figure 4.25: Losses in the transformer model

4.5 short circuit test with shunt core

The frequencies in the incoming line current to the transformer are taken from the reference description of the particular physical transformer.

Table 4.8: Frequency based short circuit test

Frequency(Hz)	Current(A)	Voltage(V)
50	138	201
250	9	66
350	7	72
1800	5	264
1900	7	385
2100	6	361
2200	5	315

Short circuit test is performed to know the working conditions impedance and losses in the system. A near full load condition is simulated and copper losses are noted .

Table 4.9: Frequency based short circuit test for 50Hz

Frequency(Hz)	Copper loss(W)	Main Core loss(W)	Shunt core loss(W)	Steinmetz losses
50	3380	80	138	8.8
250	14.7	5.89	13.6	0.625
350	8.9	6.51	15.21	0.6735
1800	4.75	64.164	139.44	3.77
1900	9.2575	137.98	298.59	7.84
2100	6.84	122.62	263.27	6.5
2200	4.53	88.369	189.03	4.5

4.5.1 For all frequencies superimposed

Table 4.10: Cumulative effect of the frequencies

Copper losses(W)	Main Core loss(W)	Shunt core losses(W)
3436.4	505.5	1057.13

4.6 short circuit test without shunt core

Table 4.11: Frequency based short circuit test

Frequency(Hz)	Current(A)	Voltage(V)
50	138	49
250	9	16
350	7	17
1800	5	61
1900	7	94
2100	6	90
2200	5	79

Table 4.12: Frequency based short circuit test for 50Hz

Frequency(Hz)	Copper losses(W)	Core losses(W)	Steinmetz losses(W)
50	3376.8	1.5018	0.89
250	14.938	0.1	0.02
350	8.61	0.1	0.025
1800	4.19	1	0.096
1900	8.9426	2.38	0.218
2100	6.71	2.16	0.18
2200	4.71	1.66	0.18

4.6.1 For all frequencies superimposed

Table 4.13: Total losses

Copper losses(W)	Core losses(W)	Steinmetz losses(W)
3424.1	8.9018	1.609

4.6.2 Comparison of results with the physical test

Table 4.14: Loss Comparison to physical test results

Core loss from simulation	Core loss from test	Difference in Percentage
4999.03	3810	31.2 %
3941.9	3810	3.4 %

5

Conclusion

A generic framework for the working model for the specific type of transformer is modelled during the span of this work, achieving the major objectives with multiple usage and diverse applications. As an initial and almost representation of real life transformer, the results are almost comparable to the available results. The deviations in the resulting values are a result of different harmonic frequencies considered for the operation. The inductance calculation and the heat modelling was the challenging part of this model setup. The model was tried with the time domain simulations to see the waveforms of the resulting voltage and currents also, it worked during the initial steps but with the increase in complexity of multiphysics it was significantly time consuming. As many parameters were assumed during this modelling, the accuracy of the model can be improved by having the exact material properties and a detailed simulation study can be set for each component. This detailed simulation might also include the 2D model of the defined parts. Refining the mesh of the model to the a finer value will also be helpful in exact calculation of losses. Strong computation system can be required as the complexity of the model increases which leads to Higher computational time as well as high computational memory.

The model can also be developed into a application by the use of application builder feature in COMSOL Multiphysics. This will hide the background details and takes only the essential inputs to produce the required results. This will also save plenty of manual input parameters as we can interrelate a few variables and make the usage more efficient and interactive to use.

Bibliography

- [1] Hasan, Syafruddin and Taib, Soib and Hardi, Surya and A. Rahim A.R and Shukri, Ahmad. Core loss characteristics analysis of power transformer under different frequencies excitation
- [2] E. I. Amoiralis, M. A. Tsili and A. G. Kladas, "Transformer Design and Optimization: A Literature Survey," in *IEEE Transactions on Power Delivery*, vol. 24, no. 4, pp. 1999-2024, Oct. 2009, doi: 10.1109/TPWRD.2009.2028763.
- [3] Tang, Q. and Wang, Z. D. and Jarman, P. *2012 IEEE International Conference on Condition Monitoring and Diagnosis*. [Electrical steels and power transformer cores in deep saturation.] 2012. 10.1109/CMD.2012.6416333.
- [4] Valkovic, Z. *IEEE Transactions on Magnetics* [Influence of transformer core design on power losses.] 2012. 10.1109/TMAG.1982.1061824.
- [5] Freitag, Christian and Leibfried, Thomas. *IEEE Transactions on Magnetics* [2017 International Conference on Optimization of Electrical and Electronic Equipment (OPTIM) 2017 Intl Aegean Conference on Electrical Machines and Power Electronics (ACEMP).] 2017. 10.1109/OPTIM.2017.7974963.
- [6] Daut, I. and Hasan, Syafruddin and Taib, Soib and Chan, Risnidar and Irwanto, M. *IEEE Transactions on Magnetics* [2010 4th International Power Engineering and Optimization Conference (PEOCO).] 2010. 10.1109/PEOCO.2010.5559192.
- [7] Lin, K.C. and Jong-Sen Hsu *Proceedings:Electrical Electronics Insulation Conference and Electrical Manufacturing Coil Winding Conference* [Selection of silicon steel for transformer cores.] 1995. 10.1109/EEIC.1995.482355.
- [8] O'Grady, K., Greaves, S. J. (1995). *Anomalous effects in minor hysteresis loops. IEEE transactions on magnetics* [. .] 31(6), 2794-2796.
- [9] Botelho, R. A., Diniz, S. B., Cunha, M. A. D., Brandao, L. P. (2015). Properties of NGO 3 Silicon Steel Asymmetrically Cold Rolled. *Materials Research*, 18, 143-147.
- [10] Lin, K.C. and Jong-Sen Hsu. *Selection of silicon steel for transformer cores* [Proceedings:Electrical Electronics Insulation Conference and Electrical Manufacturing Coil Winding Conference .] 1995 10.1109/EEIC.1995.482355.
- [11] Reinert, J. and Brockmeyer, A. and De Doncker, R.W.A.A. *Calculation of losses in ferro- and ferrimagnetic materials based on the modified Steinmetz equation* [IEEE Transactions on Industry Applications .] 2001 10.1109/28.936396.
- [12] M. Irving and P.E. Gottlieb *An overview of transformers in electrical technology* [Practical Transformer Handbook.]

- [www.sciencedirect.com/science/article/pii/B9780750639927500028] 1998
doi.org/10.1016/B978-075063992-7/50002-8
- [13] Shozaburo Nakashima and Kunihide Takashima and Jiro Harase *Effect of Silicon Content on Secondary Recrystallization in Grain-oriented Electrical Steel Produced by Single-stage Cold Rolling Process [ISIJ International.]* 1991 10.2355/isijinternational.31.1007
- [14] Venkatachalam, Kapil and Sullivan, Charles R and Abdallah, Tarek and Tacca, Hern *2002 IEEE Workshop on Computers in Power Electronics, 2002. Proceedings.* 2002. 10.1109/PEOCO.2010.5559192.
- [15] G. Paoli, O. Biro and G. Buchgraber, "Complex representation in nonlinear time harmonic eddy current problems," in *IEEE Transactions on Magnetics*, vol. 34, no. 5, pp. 2625-2628, Sept. 1998, doi: 10.1109/20.717607.
- [16] Flegar, I, "Some general properties of power electronic conversion networks," in *Archiv für Elektrotechnik*, vol. 68, no. 5, pp. 365-372, Sept. 1985,
- [17] Elshaharty, Mohamed Atef and Luna, Alvaro and Candela, Jose Ignacio and Rodriguez, Pedro, "A unified power flow controller using a power electronics integrated transformer," in *IEEE Transactions on Power Delivery*, vol. 34, no. 3, pp. 828-839, 2019,
- [18] Dasgupta, Sukanya and Biswas, Sujit K, "Three-phase Sine Wave Inverter using Natural Harmonic Compensation," in *2020 IEEE Calcutta Conference (CALCON)*, pp. 521-525, 2020
- [19] Firdoush, Shahina and Kriti, Shruti and Raj, Avinow and Singh, Shusant Kumar, "Reduction of Harmonics in Output Voltage of Inverter," in *International Journal of Engineering Research & Technology (IJERT)*, vol. 4, no. 2, pp. 1-6, 2016
- [20] Yan Hu, Renyuan Tang, Xiulian Wang, Liangyun Zhao and Zhenyan Guo, "The analysis and calculation of the magnetic flux density distributions in a 3-phase roll-iron core transformer," *Sixth International Conference on Electrical Machines and Systems*, 2003. ICEMS 2003., 2003, pp. 790-793 vol.2.
- [21] Quach, D. T., Pham, D. T., Ngo, D. T., Phan, T. L., Park, S. Y., Lee, S. H., Kim, D. H. (2018). Minor hysteresis patterns with a rounded/sharpened reversing behavior in ferromagnetic multilayer. *Scientific reports*, 8(1), 1-9.
- [22] <https://www.comsol.se/model/effective-nonlinear-magnetic-curves-calculator-30941>

A

Appendix 1

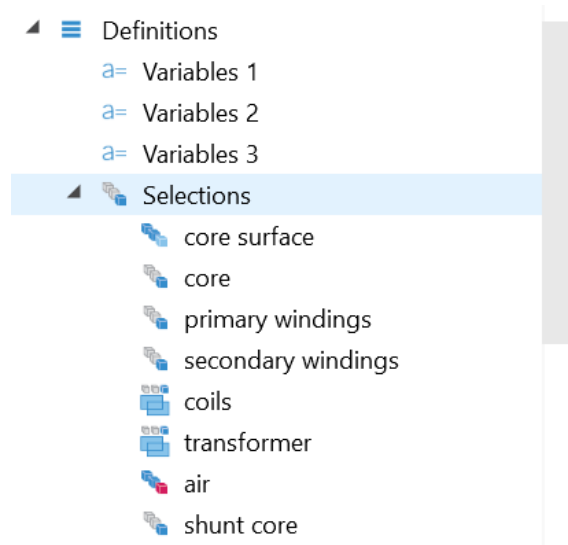


Figure A.1: Selection of transformer components

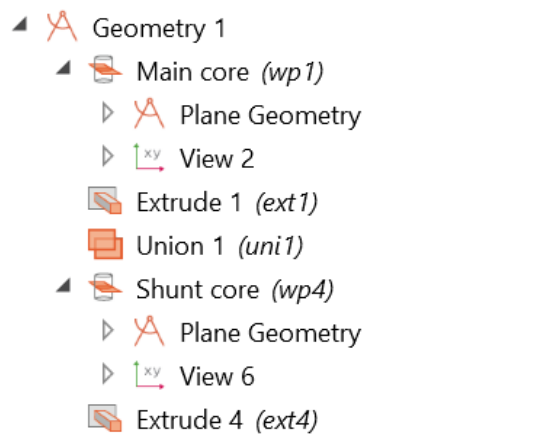


Figure A.2: Geometry steps for main and shunt core

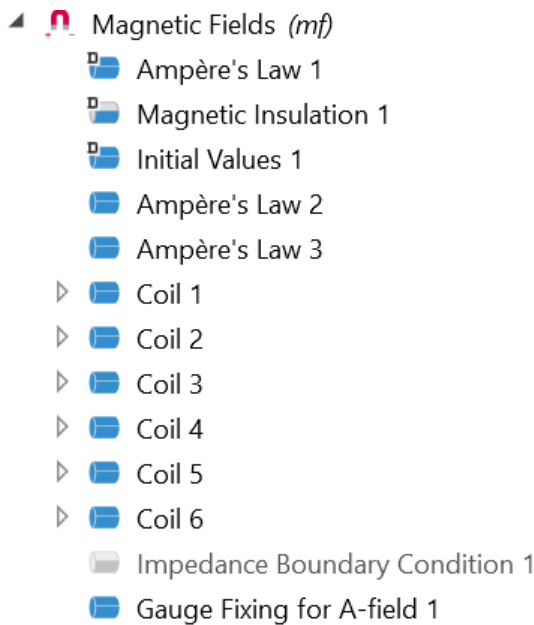


Figure A.3: Details of magnetic field interface

»	Property	Variable	Value	Unit	Property group
<input checked="" type="checkbox"/>	Relative permeability	mur_is...	1	1	Basic
<input checked="" type="checkbox"/>	Heat capacity at constant pressure	Cp	385[J/(kg*K)]	J/(kg·K)	Basic
<input checked="" type="checkbox"/>	Relative permittivity	epsilon...	1	1	Basic
<input checked="" type="checkbox"/>	Density	rho	8940[kg/m^3]	kg/m³	Basic
<input checked="" type="checkbox"/>	Thermal conductivity	k_iso ;...	200[W/(m*K)]	W/(m·K)	Basic
	Electrical conductivity	sigma_i...	5.998e7[S/m]	S/m	Basic
	Surface emissivity	epsilon...	0.5	1	Basic
	Young's modulus	E	126e9[Pa]	Pa	Young's modulus and
	Poisson's ratio	nu	0.34	1	Young's modulus and
	Reference resistivity	rho0	1.667e-8[ohm*m]	Ω·m	Linearized resistivity
	Resistivity temperature coefficient	alpha	3.862e-3[1/K]	1/K	Linearized resistivity
	Reference temperature	Tref	293.15[K]	K	Linearized resistivity

Figure A.4: Copper properties

»	Property	Variable	Value	Unit	Property group
✓	Relative permeability	mur_is...	1	1	Basic
✓	Relative permittivity	epsilo...	1	1	Basic
✓	Electrical conductivity	sigma_...	0[S/m]	S/m	Basic
✓	Heat capacity at constant pressure	Cp	Cp(T)	J/(kg·K)	Basic
✓	Density	rho	rho(pA,T)	kg/m ³	Basic
✓	Thermal conductivity	k_iso ;...	k(T)	W/(m·K)	Basic
	Coefficient of thermal expansion	alpha_i...	alpha_p(...	1/K	Basic
	Mean molar mass	Mn	0.02897[...	kg/mol	Basic
	Bulk viscosity	muB	muB(T)	Pa·s	Basic
	Dynamic viscosity	mu	eta(T)	Pa·s	Basic
	Ratio of specific heats	gamma	1.4	1	Basic
	Speed of sound	c	cs(T)	m/s	Basic
	Refractive index, real part	n_iso ;...	1	1	Refractive index
	Refractive index, imaginary part	ki_iso ;...	0	1	Refractive index
	Parameter of nonlinearity	BA	(def.gam...	1	Nonlinear model

Figure A.5: Air properties

»	Property	Variable	Value	Unit	Property group
✓	Electrical conductivity	{sigma...	{500[S/...	S/m	Basic
✓	Relative permittivity	epsilo...	1[1]	1	Basic
✓	Relative permeability	mur_is...	8500	1	Basic
✓	Heat capacity at constant pressure	Cp	812	J/(kg·K)	Basic
✓	Density	rho	6000	kg/m ³	Basic
✓	Thermal conductivity	k_iso ;...	34	W/(m·K)	Basic
	Magnetic flux density norm	normB	BH(norm...	T	B-H curve
	Magnetic field norm	normH	BH_inv(n...	A/m	B-H curve
	Magnetic coenergy density	Wpm	BH_prim(...	J/m ³	B-H curve
	Effective magnetic flux density n...	normB...	BHeff(no...	T	Effective B-H curve
	Effective magnetic field norm	normH...	BHeff_in...	A/m	Effective B-H curve

Figure A.6: Silicon properties

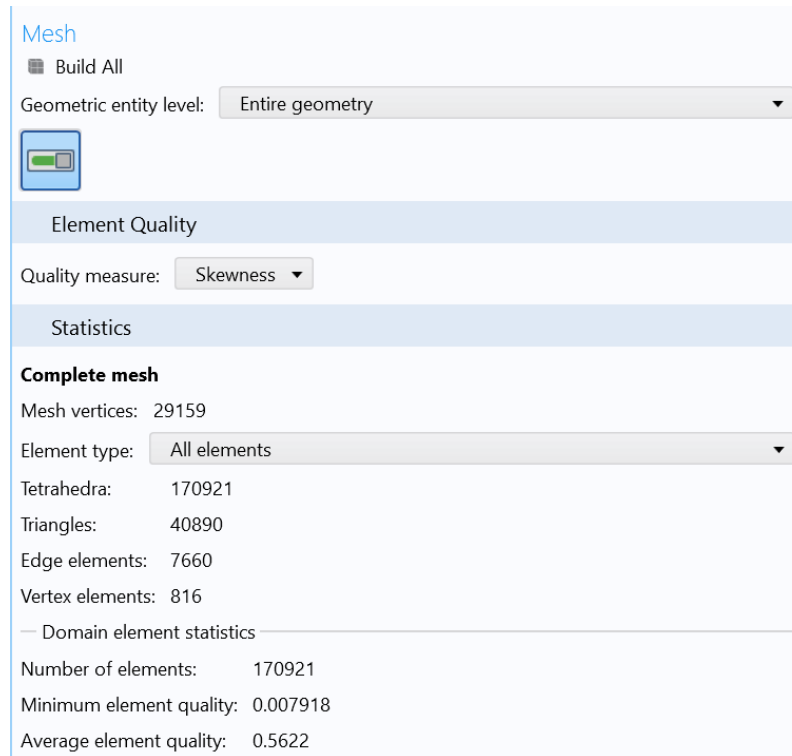


Figure A.7: Mesh statistics

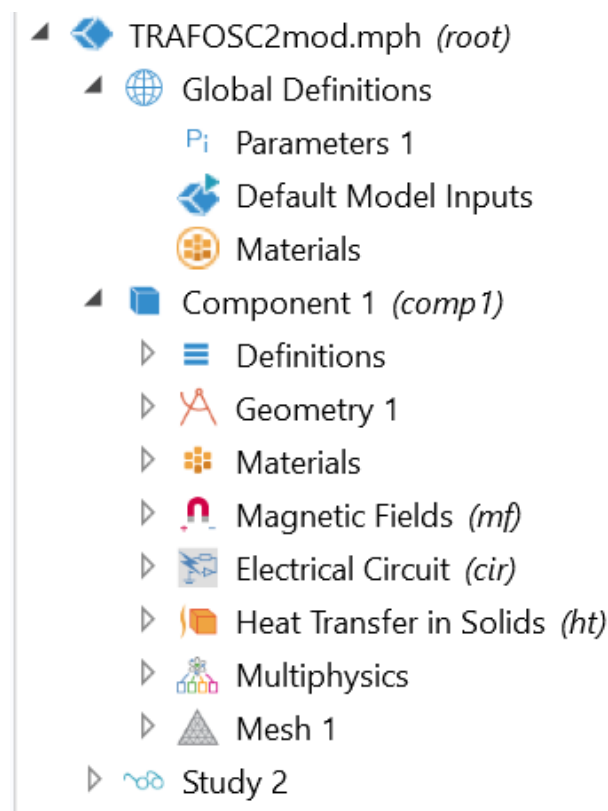


Figure A.8: Overall steps

DEPARTMENT OF SOME SUBJECT OR TECHNOLOGY
CHALMERS UNIVERSITY OF TECHNOLOGY
Gothenburg, Sweden
www.chalmers.se



CHALMERS
UNIVERSITY OF TECHNOLOGY